Water Science & Technology

Water Science & Technology Vol 84 No 10-11, 3286 doi: 10.2166/wst.2021.430

Unlocking the potential of biosynthesized zinc oxide nanoparticles for degradation of synthetic organic dyes as wastewater pollutants

Jaya Gangwar and Joseph Kadanthottu Sebastian*

Department of Life Sciences, Christ University, Bangalore, Karnataka, India
*Corresponding author. E-mail: joseph.ks@christuniversity.in

JG, 0000-0001-7038-8547; JKS, 0000-0003-4384-2462

ABSTRACT

The azo dyes released into water from different industries are accumulating in the water bodies and bioaccumulating within living systems thereby affecting environmental health. This is a major concern in developing countries where stringent regulations are not followed for the discharge of industrial waste into water bodies. This has led to the accumulation of various pollutants including dyes. As these developing countries also face acute water shortages and due to the lack of cost-effective systems to remove these pollutants, it is essential to remove these toxic dyes from water bodies, eradicate dyes, or generate fewer toxic derivatives. The photocatalysis mechanism of degradation of azo dyes has gained importance due to its eco-friendly and non-toxic roles in the environment. The zinc nanoparticles act as photocatalysts in combination with plant extracts. Plant-based nanoparticles over the years have shown the potential to degrade dyes efficiently. This is carried out by adjusting the dye and nanoparticle concentrations and combinations of nanoparticles. Our review article considers increasing the efficiency of degradation of dyes using zinc oxide (ZnO) nanoparticles and understanding the photocatalytic mechanisms in the degradation of dyes and the toxic effects of these dyes and nanoparticles in different tropic levels.

Key words: azo dyes, dye degradation, green synthesis, nanoparticle, toxicity, water pollution

HIGHLIGHTS

- The review focuses on green synthesis of metallic ZnO nanoparticles.
- Dye degradation by greener and cost-effective approach is the need for many developing countries.
- Green synthesised ZnO nanoparticle photocatalysis mechanism is reviewed comprehensively.
- Toxicity of dyes and ZnO nanoparticles at tropic levels is highlighted.

INTRODUCTION

The rapid increase of population affects the availability of pure and clean water. The pollutants and dyes become bioaccumulated in water bodies and the environment because of the release of pollutants into the nearby water bodies without any pre-processing and degradation. This has become a major concern for developing countries. The need to use safe and clean water leads us to approach methods of getting clean water (Brame *et al.* 2011; Jain *et al.* 2021).

Nanoparticles have many applications in the field of cosmetics, medicine, and wastewater management, etc. Nanoparticles can be synthesized from synthetic and biological sources with different elements such as silver, gold, copper, zinc, iron, etc. The chemical methods include two methods as: the bottom-up and top-down approaches which are costly and toxic. To cut down the expenses and reduce toxic effects, researchers have approached green synthesis methods (Agarwal *et al.* 2017). The biological sources for the generation of nanoparticles include the synthesis of nanoparticles from microorganisms, fungi, plants, etc. via phytochemicals. The phytochemicals consist of polyphenols, terpenoids, quinine, proteins, saponins, and alkaloids (Figure 1(a)). The phytochemicals are found in different parts of medicinal plants, fruits, nuts, cereals (Kurmukov 2013). These phytochemicals have many applications such as antibacterial, antiviral, catalytic properties, and many more. It also provides a route for the biosynthesis of nanoparticles through the green approach.

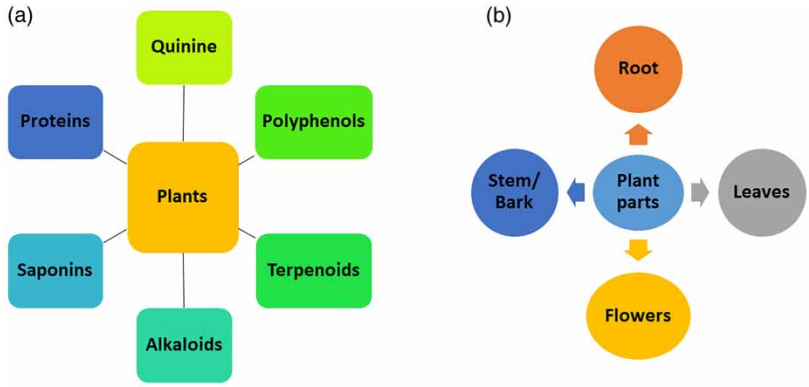

Figure 1 | Phytochemicals present in medicinal plants and different plant parts used in the synthesis of nanoparticles.

Azo dyes are toxic due to their functional groups, which can be degraded using different methods, which include physical, chemical, and biological methods. The physical techniques comprise adsorption, filtration, and ultraviolet (UV) light irradiation. The chemical methods include chemicals that degrade toxic dyes, and mechanisms that consist of oxidation processes with hydrogen peroxide and hypo chloride. The biological techniques involve microorganisms, fungi, algae, and plants (Saini 2017). As microorganisms are easy to handle and genetic manipulation can be done in species like *Bacillus,* these can be used to synthesize zinc oxide nanoparticles which can help in the degradation of textile dyes and exhibit antimicrobial activity (Rehman *et al.* 2019).

In this review article, we have focused on the extraction process of biosynthesized ZnO nanoparticles (NPs) using extracts of plants and microorganisms. As phytochemicals, microbial enzymes act as a reducing agent in the synthesis of nanoparticles. The review also focuses on the mechanism of photocatalytic dye degradation and how the adsorption of dyes is related to the degradation of dyes. It concentrates on the mechanism of toxicity of ZnO nanoparticles and their effects when they enters the different tropic levels like an aquatic ecosystem.

PROPERTY AND SYNTHESIS OF ZnO NANOPARTICLES

ZnO nanoparticles have a wide range of applications due to their semiconducting, piezoelectric, and pyroelectric properties. This is due to their large band gap and high binding energy and hence have been used in optics, electronics, biomedical, agricultural, and environmental remediation.

PROPERTY OF ZnO NANOPARTICLES

ZnO has optoelectronics applications and semiconductor applications due to its wide band gap $Eg \sim 3.3$ eV at 300 K. The ZnO crystal exists as wurtzite, zinc blende, and rock salt. ZnO exists in ambient conditions on cubic substrates and at high pressures, as wurtzite, zinc-blende, and rock salt, respectively (Özgür *et al.* 2005). The electronic structure of the thermostable phase of ZnO in the wurtzite structure exists in an sp^3 hybridization with each Zn atom surrounded by four neighboring O atoms at corners of a tetrahedron shape (Feng *et al.* 2013). ZnO nanoparticles act as semiconductors, photocatalysts due to their high energy gap and ferromagnetic properties (Garcia *et al.* 2007; Hong *et al.* 2009; Nair *et al.* 2011). ZnO nanoparticles can be doped with transition metals like manganese, nickel, and cobalt to generate different nanostructures like nanofilms, nanotubes, and nanobelts (Djurišić & Leung 2006). ZnO nanoparticles, which are generated by the CTAB-assisted hydrothermal process, exist as nanoflowers, nanoswords, and nanoneedle-like structures due to the interaction of cationic detergent and ZnO nuclei. At low temperatures (120 °C), the nanoparticles exist as nanorods, as temperature is increased from 120 °C to 160 °C, the shape changes from nanorods to nanoneedle-like structures and nanoflowers and nanoswords exist at low temperatures (Zhang *et al.* 2004).

BIOSYNTHESIS OF ZnO NANOPARTICLES USING PLANTS AND ITS PHOTOCATALYTIC DEGRADATION OF DYES

The Nanoparticles can be synthesized by conventional and non-conventional methods. The Traditional methods can be expensive, toxic in nature, and non-ecofriendly. Whereas in the biological approach, the phytochemical acts as a reducing

and capping agent, is more efficient, resulting in preservation of raw materials for a longer time, specifically plants consist of higher contents of phytochemicals which can inhibit the synthesis of nanoparticles (Singh *et al.* 2021). The synthesis of nanoparticles can be optimized by controlling the reaction time, pH, and temperature of the reaction. The extraction methods followed for the synthesis of nanoparticles use phytochemicals present inside plants and are depicted in Table 1. The nanoparticles can be synthesized using different plant parts like root, leaves, flower, stem, and barks (Figure 1(b)).

DEGRADATION OF DYES FROM ZnO NANOPARTICLES SYNTHESIZED FROM PLANTS

Numerous plants and their phytochemicals have been utilized as reducing agents for the degradation of dyes (Table 2). The phytochemicals present in these plants can degrade azo dyes with an efficiency of 80%–90%. *Moringa oleifera* leaf extracts with ZnO have been utilized in the degradation of titan yellow with an efficiency of 96% (Pal *et al.* 2018). However, few plants are as efficient in degrading dyes. In leaf extracts of *Sageretia*, the synthesized ZnO nanoparticles degraded crystal violet under UV light, which was highest (40.65%), followed by in the dark (37%) and in light (36.45%) (Talha Khalil *et al.* 2019).

SYNTHESIS OF ZnO NANOPARTICLES VIA MICROORGANISMS

The Nanoparticles are biosynthesized from microorganisms like algae, bacteria, and fungi. The bacterial, algal, and fungal enzymes help in the biosynthesis of nanoparticles and act as reducing agents. Algae like *Sargassum, Cladophora, Chlamydomonas,* and *Garcilaria* have been utilized for the synthesis of ZnO particles (Table 3). Bacteria like *Arthrospira platensis, Lactobacillus sporogens*, *Pseudomonas aeruginosa*, *Bacillus haynesii, Bacillus licheniformis, Halomonas elongate, Aeromonas hydrophila,* and *Bacillus* sp. have been utilized. *Penicillium chrysogenum, Trichoderma harzianum,* marine yeast*, Cochliobolus geniculatus, Aspergillus terreus, Phanerochaete chrysosporium, Periconium* sp., and *Pichia kudriavzevii* species of fungi also have been utilized for the synthesis of ZnO nanoparticles (Table 3).

DEGRADATION OF DYES FROM ZnO NANOPARTICLES SYNTHESIZED BY MICROORGANISMS

Biodegradation of dyes using microorganisms is becoming increasingly popular due to the easy availability, cost-effective nature, and ease of growth under laboratory conditions. However, one of the significant reasons for the biological synthesis of ZnO nanoparticles is the existence of biologically active metabolites or enzymes that could be engaged as reducing agents during dye degradation (Khanna *et al.* 2019. Several dyes like methylene blue, methylene orange, have been degraded by ZnO nanoparticle synthesis using algae, bacteria, and fungi (Table 4).

ORGANIC DYES PRESENT IN WATER BODIES AND MECHANISM OF TOXICITY

The azo dyes are synthetic organic dyes with an azo functional group. Azo dyes are grouped into different classes as reactive dyes, disperse dyes, acidic dyes, basic dyes, direct dyes, vat dyes, sulfur dyes, and solvent dyes (Saratale *et al.* 2011; Madhushika *et al.* 2020). The synthetic dyes consist of 70% azo dyes in the textile, food, cosmetics industries, etc. Azo dyes are toxic in nature, acting as carcinogens, genotoxins and mutagens (Ventura-camargo & Marin-morales 2013) (Table 5).

Textile dyes get mixed with industrial pollutants and are highly toxic and carcinogenic. These dyes are also toxic to the biological treatment units, thereby making the treatment of these dyes extremely complex (Tunçal & Kaygusuz 2014). The toxic dyes accumulate in sediments and soil, which then transport the water systems. The dyes assimilate in fish gills and accumulate in tissues. The azo dyes of chromium complexes damage the growth and development of plants (Lellis *et al.* 2019). The UV or chlorination process is efficient in degrading dyes from wastewater, but it has not been used in water bodies like ponds and lakes (Nikravesh *et al.* 2020). The toxic effects of dyes can be observed in aquatic animals like *Xenopus laevis* and *Danio rerio* (zebrafish) and can cause developmental stage and embryonic damage, respectively. *Xenopus laevis* tadpoles at the 46th stage of development were exposed to six textile dyes, mainly Astrazon Red, Astrazon Blue, Remazol Red, Remazol Turquoise Blue, Cibacron Red, and Cibacron Blue FN-R for 168 h in static conditions. The dyes caused oxidative stress, and the presence of organic pollutants caused increased levels of the glutathione *S*-transferase (GST) enzyme. The exposure of fishes to Metanil yellow causes increased GST enzyme activity in the liver and intestinal tissues (Güngördü *et al.* 2013). Zebrafish were exposed to textile dyes such as Maxilon blue 5G and Reactive blue 203 for 96 h, which caused acute toxicity and embryonic damage. The dyes have induced DNA damage and deformities in fish like curved body axis, tail malformation, and reproductive damage. Limited studies have been done on the mechanism of DNA damage caused by textile dyes (Köktürk *et al.* 2021). The toxic effects of textile dyes (Optilan yellow, Drimarene blue, and Lanasyn

Table 1 | Methodology of synthesis of ZnO nanoparticles from plants

Common name	Scientific name	Extraction method	Phytochemicals	Reference
Red fruit passion flower	*Passiflora foetida*	25 g of peel powder with 200 mL water in a beaker and stirred for 30 min at 70 °C. The solution is passed through Whatman filter paper no. 42 and centrifuged at 7,000 rpm.	Saponins, tannins, steroids, terpenoids, flavonoids	Khan *et al.* (2021), Siriwardhene (2013)
Date palm	*Phoenix dactylifera*	Syrup washed to eliminate dirt room dried for 36 h, powdered and sieved through 100 mesh.	Quinones, organic acids, and flavones	Rambabu *et al.* (2021)
Miracle grass	*Gynostemma pentaphyllum*	5 g of dry plant powder was added to a conical flask with 100 mL distilled water. Then it was autoclaved for 40 min at 100 °C with high pressure. The autoclaved extract was filtered with Whatman No. 1 filter paper and centrifuged at 4,500 rpm at room temperature for 15 min to eliminate undesired components.	Flavonoid, quercetin, alkaloids, rutin	Park *et al.* (2021)
Bush plum	*Carissa edulis*	10 mg of extract in 20 mL of water mixed with 80 mL of 1 mM of zinc nitrate to synthesis ZnO NPs.	Alkaloids, sterols, resin	Fowsiya *et al.* (2016)
Thick-leaf lavender	*Anisochilus carnosus*	Leaves extract allowed to boil using a stirrer heater. Then, 5 g of zinc nitrate was added to the above solution as the temperature reached 60 °C. This mixture was further boiled until its color changed into a dark yellow.	Polyphenols, carboxylic acid, polysaccharides, amino acids, and proteins	Anbuvannan *et al.* (2015)
Redbush tea	*Aspalathus linearis*	The natural extract was used to reduce zinc-based salts including $ZnNO_3$, and $ZnCl_2$, as well as Zn-ammonium hydrate-based precursors.	Flavones, flavanones and flavonols	Diallo *et al.* (2015)
Indian borage	*Plectranthus amboinicus*	0.1 M zinc nitrate solution was prepared with 30 ml water. Then 10 ml *P. amboinicus* leaf extract was added to the above solution and kept under continuous stirring at 80 °C for 4 h.	Saponins, polyuronides (pectins, mucilage, gums), tannins (gallic), reducing compounds, flavonoids	Fu & Fu (2015)
Maakada singi	*Caralluma fimbriata*	1 mol% leaves extract, and an aqueous mixture of zinc nitrate was added to gadolinium nitrate solution with constant stirring to ensure uniform mixing. The Petri dish containing the redox mixture was placed into a muffle furnace maintained at 350 $\pm$ 10 °C.	Alkaloids, flavonoids, carbohydrates, glycosides, sterols, saponins, oils and fats, tannins, phenolic compounds, proteins and amino acids, gums and mucilage	Mishra *et al.* (2016), Packialakshmi & Naziya (2014)
Autumn joy	*Sedum alfredii*	30 g of Shoots of *S. alfredii* were mixed in 95% ethanol solution at 70 °C for 120 min after particles adhering to the surfaces of the shoots had been removed with water. The mixtures were filtered 3 times with filter paper. The residues and filtrates were collected, respectively. NaOH	Chlorophyllin	Wang *et al.* (2016)

(*Continued.*)

Table 1 | Continued

Common name	Scientific name	Extraction method	Phytochemicals	Reference
		(10%) was added to the filtrates to adjust the pH values to 11.		
Pecan	*Carya illinoinensis*	10 g of leaves are cut into pieces, ground into a paste, and soaked in 100 mL of deionized water in a 250 mL glass beaker. The solution was heated at 70 °C for 30 min using a magnetic stirrer until the color of the solution changed. The aqueous leaf extract was left to cool down at room temperature, filtered using Whatman No. 1 filter paper, and centrifuged at 7,000 rpm for 30 min.	Total phenolics (TP), condensed tannin (CT)	Ahmad *et al.* (2021), Villarreal-Lozoya *et al.* (2007)
Olive	*Olea europaea*	10 g of *O. europaea* leaves were mixed with 100 ml of deionized water. The mixture was heated at 60 °C for 30 min using a stirrer heater. The resulting product was filtered.	Terpenoids, phenolic compounds, flavonoids, and alkaloids	Hashemi *et al.* (2016)
Thyme	*Thymus vulgaris*	6 g in 100 mL distilled water (DW), heating at 80 °C for 1 h, and then filtered.	Thymol, carvacrol	Weldegebrieal (2020)
Moringa	*Moringa oleifera*	5 g of leaves were washed thoroughly with distilled water, and the surfaces of leaves were sterilized using alcohol. These leaves were heated for 40 min in 100 ml of distilled water at 50^0 C. Then, the extract was filtered with Whatman No. 41 filter paper.	Alkaloids, glycosides, phenols, saponins, tannins, volatile oils, and hydrolyzable tannins.	Pal *et al.* (2018), Dahiru *et al.* (2006)
Aloe vera	*Aloe barbadensis miller*	Small pieces of peel were cut and grounded with pestle mortar in distilled water to make an aqueous solution of peel extract. The aqueous solution was filtered with Whatman filter paper No. 1 to remove debris.	Tannins, saponins, flavonoids,	Weldegebrieal (2020)
Okra	*Abelmoschus*	10 mL of leaves mixed in 0.01 mol zinc acetate dihydrate was hydrolyzed with the 0.01 mol sodium hydroxide with the leaf extract, pH is adjusted to the basic at 9–11, then cool at room temperature. Centrifuge at 7,000 rpm for 10 min.	Steroids, terpenes, alkaloids, flavones, lignins	Mirgane *et al.* (2020), Chaudhary *et al.*(2019)
Eucalyptus	*Eucalyptus globulus*	20 g of leaf powder was added to 100 ml of deionized water and kept for boiling at 80^0 C for about 1 h. The formed precipitate was filtered, and obtained supernatant was stored at 4 °C.	Cuminic aldehyde	Siripireddy & Mandal (2017)
Neem	*Azadirachta indica*	25 g of fresh leaves in 100 mL of double-distilled water (DDW), heating while stirring at 60 °C for 20′ and then filtered.	Alkaloids, flavonoids, saponins, reducing sugars	Weldegebrieal (2020)
Coriander	*Coriandrum sativum*	10 g Coriander leaf powder was dissolved in 100 ml of distilled water and stirred at 100 °C for 15 min. The solution was then filtered with a 1.5-micron Whatman filter paper No. 1.	Flavonoids, saponins, carbohydrates, phenol	Singh *et al.* (2019)
Oak	*Quercus* L.		Steroids, terpenes, alkaloids, flavones, lignins	Sorbiun *et al.* (2018)

		20 g of fruit was added in 100 mL of distilled water and boiled for 5 min. after boiling, the color of the aqueous solution was dark brown, and the mixture was allowed to cool to room temperature.		
Mangosteen	*Garcinia mangostana*	8 g of fruit pericarps in 100 mL water, heated at 70–80 °C for 20 min and then filtered.	Phenolic acids, flavonoids, alkaloids, triterpenoids	Weldegebrieal (2020)
Dhobi tree	*Mussaenda frondosa*	Plant extract and distilled water in the ratio (1:10) were taken in a round-bottomed flask, and the extraction was carried out at 100 °C under reflux for 4 h. The extract was filtered through Whatman filter paper No. 1 and centrifuged to remove any undissolved debris	Alkaloids, flavonoids, tannins, glycosides	Jayappa *et al.* (2020), Pappachen & Sreelakshmi (2017)
Dane wort	*Sambucus ebulus*	2 mL of extract mixed with a solution for 2 h at 80 °C; the suspension was centrifuged for 15 min, and the precipitate was dried at 60 °C.	Acetic acid, pentatonic acid, lignocaine, isovaleric acid	Alamdari *et al.*(2020)
Simple leaf chaste tree	*Vitex trifolia*	40 g leaves were boiled with 200 ml of double-distilled water for 40 min at 60^0 C. Mild yellow-colored solution is formed, once cooled at room temperature it was filtered with filter paper (Whatman No. 1).	Alkaloids, saponins, tannin, phenols, terpenoids, flavonoids, and steroids	Elumalai *et al.* (2015)
Broccoli	*Brassica oleracea* L. var. *italica*	8 g of the dried broccoli was weighed out, washed with double deionized water to eliminate superficial impurities. The pulverized broccoli was mixed with 80 mL of deionized water and heated at 70 ˚C for 20 min.	Polyphenols and flavonoids	Osuntokun *et al.* (2019)
Pinwheel flower	*Tabernaemontana divaricata*	60 mL of leaf extract was heated to 80 ˚C and kept stirring, and 6 g of zinc nitrate was added to this solution at 80 ˚C. This mixture was boiled until a yellow-colored paste was formed.	Carbohydrates, glycosides, amino acids, flavonoids, tannins, alkaloids, and steroids,	Raja *et al.* (2018), Jain *et al.* (2010)
Hyacinth bean	*Dolichos lablab* L.	20 g of leaves were weighed and heated in 100 ml of Milli-Q water at 70 °C for 30 min. The extract was allowed to cool and then filtered with Whatman No. 42 filter paper to produce greenish-yellow filtrate.	Alkaloids, flavonoids, tannins, glycosides	Kahsay *et al.* (2019)
Sea buckthorn	*Hippophae rhamnoides*	5 g of fruit mixed with 100 mL of water. Powdered fruit was treated using a high-pressure autoclave at 100 °C for 1 h. Autoclaved extracts were filtered using Whatman No. 1, 110 mm filter paper.		Rupa *et al.* (2019)
Hemp	*Cannabis sativa*	10 g of shade-dried leaves were crushed and added to 100 ml of deionized water in a 250 ml conical flask. The hot water bath was set at 60 °C for 12 h.		Chauhan *et al.* (2020)
Pine spurge	*Euphorbia prolifera*	50 g of dried leaves powdered was added to 250 mL double-distilled water in a 500 mL flask and mixed. The preparation of extract was using a magnetic heating stirrer at 70 °C for 30 min.	Phenols	Momeni *et al.* (2016)
Piper betel	*Betel*	Water was added to the leaf extract in the 1:3 ratio and boiled at 800 °C for 45 min. The solution is cooled at	Alkaloids, tannins, phenolic compound, flavonoid, steroids glycosides, terpenes, anthraquinones	Rajesh *et al.* (2016)

(*Continued.*)

Table 1 | Continued

Common name	Scientific name	Extraction method	Phytochemicals	Reference
		room temperature for 6 h. Zinc acetate was taken (0.1 M) and added to the water.		
Basil	*Ocimum basilicum*	Leaves of the plant were extracted with ethanol by maceration.	Rosmarinic acid, flavionoids	Fathiazad *et al.* (2012)
Roselle	*Hibiscus sabdariffa*	An aqueous solution of flowers is prepared and left to stir for 2 h. The mashes were placed in a water bath at 60 °C for 1 h and filtered with Whatman No. 4 filters.	Phenolic, flavonoids	Soto-Robles *et al.* (2019)
Chinaberry	*Melia azedarach*	20 g of leaves in 125 mL of DDW subjected to Soxhlet extraction for 72 h and then filtered.	Terpenoids, flavonoids, steroids, alkaloids	Weldegebrieal (2020)
Baikal skullcap	*Scutellaria baicalensis*	5 ml of plant extract mixed with 95 ml of distilled water make up to 100 ml water. This combination was mixed with zinc nitrate heated to 75 °C for 1.5 h.		Chen *et al.* (2019)
Jujube	*Ziziphus jujuba*	100 ml jujube extract was drop-wisely added to 25 mL $Zn(NO_3)_2.6H_2O$ aqueous solution of 0.05 M, and the mixture was vigorously stirred at room temperature for 30 min.	Triterpenic acids, cerebrosides, flavonoids, phenolic acids, amino acids, polysaccharides	Golmohammadi *et al.* (2020)
Red powder puff	*Calliandra haematocephala*	Air-dried leaves were mixed with water in a 1:20 weight proportion and were heated in a dry-bath at 80 °C for 15 min, to yield a thin pale-yellow soup of the leaf extract	Caffeic acid and myricitrin	Vinayagam *et al.* (2020)
Desert horsepurslane	*Trianthema portulacastrum*	10 ml of leaf extract was mixed with 25 mL of $ZnSO_4$ in a 150 mL beaker at 25 °C.		Khan *et al.* (2019)
Star fruit	*Averrhoe carrambola*	0.5 M zinc nitrate solution was prepared with 50 mL distilled water. The plant extract was added to zinc nitrate in a ratio of 9:1 under continuous stirring.	Oxalic acid	Chakraborty *et al.* (2020)
Teak	*Tectona grandis*	20 g of leaves were collected, weighed, washed under tap water. Collected leaves were cut into fine fragments and placed into a round-bottomed flask with 100 ml of double deionized water. The whole reaction mixture was heated at 60 °C for 1 h and filtrate was obtained employing Whatman No. 1 filter paper.	Alkaloids, flavonoids, carbohydrates, glycosides, steroids, and tannins	Raizada *et al.* (2019)
Chinese sweet-plum	*Sageretia thea*	The aqueous solution of leaves mixed with a zinc nitrate solution.		Talha Khalil *et al.* (2019)
Rambutan	*Nephelium lappaceum* L.	Fresh peels were washed, dried at 50 °C in the oven, then 3 g in 40 mL DDW:20 mL EtOH solvent was heated at 80 °C for 10 min and then filtered.	Polyphenols, flavonoids, alkaloids, tannins, saponins (EtOH extract)	Weldegebrieal (2020)
Golden shower	*Cassia fistula*	1:10 proportion of the coarsely powdered plant material to water was taken in a round-bottomed flask, and the extraction was carried out at 100 °C with are flux arrangement for 5 h with constant stirring. The extract was filtered and centrifuged.	Polyphenols (11%) and flavonoids (12.5%)	Suresh *et al.* (2015)
Jackfruit				Vidya *et al.* (2016)

	Artocarpus heterophyllus	Zinc nitrate hexahydrate was added to the leaf extract and heated for about an hour to get a thick dark brown-colored liquid.	Terpenoids, flavonoids, phenols, steroids, glycosides, carbohydrates, and saponins	
Tomato	*Solanum lycopersicum*	Fresh tomatoes were washed, squeezed to get juice, dissolved in DDW by stirring at 30 °C for 30 min and then filtered.	Flavonoids, phenolics, carotenoids, alkaloids	Weldegebrieal (2020)
Ginger	*Zingiber officinale*	Powdered leaves in 100 mL of DW was separately boiled at 60 °C for 1 h while stirring and then filtered.	Terpenoids, phenolic acid, flavonoids, proteins	Weldegebrieal (2020)
Garlic	*Allium sativum*	Fresh and finely sliced bulbs were boiled at 70–80 °C for 20 min and then filtered.	Flavonoids, anthocyanins, vitamins (B1, B2, B6, etc.)	Weldegebrieal (2020)
Flax	*Linum Usitatissimum*	50 mL of distilled water has been added to 1 g of seeds and prepared mixture stirred for 2 h at 60 °C. The extract is filtered.		Alkasir *et al.* (2020)
Alpine almond	*Hydnocarpus alpina*	10 g of powder was taken to extract with an ethanol-water mixture (60:40) and ethanol (95%) separately.		Ganesh *et al.* (2019)
Onion	*Allium cepa*	5 g of dry brown outer onion peel were washed with tap water, followed by rinsing with distilled water and soaked in 50 mL of double-distilled water. The solution was boiled at 70 °C for 15 min. The peel broth was filtered through Whatman No. 1 paper.	Phenolic compounds, proteins, and amino acids	Rajkumar *et al.* (2019)
Parsley	*Petroselinum crispum*	20 g of fresh leaves of parsley were extracted in100 mL ultrapure water by refluxing for 60 min.	Vitamins (beta-carotene, thiamin, riboflavin, and vitamins C and E), fatty acids, volatile oils	Stan *et al.* (2015)
Loquat	*Eriobotrya japonica*	25 g of the seed powder was mixed with 100 mL deionized water. The mixture was then stirred on a magnetic hotplate stirrer at 40 °C for 60 min. Then, the supernatant was collected by Whatman No. 1 filter paper.	Phenolics, alcohols, sugars, and proteins	Shabaani *et al.* (2020)
Malabar cardamom	*Amomum longiligulare*	25 mg of powder were diluted in 100 ml of distilled water, and the suspension was autoclaved for 30 min at 100 °C to obtain an aqueous solution of extract. The extracts were centrifuged at 5,000 rpm for 10 min and filtered using Whatman No. 1 filter paper.	Essential oil	Liu *et al.* (2020)
Saffron	*Crocus sativus*	5 g of leaf powder was dissolved in 100 mL deionized water, blended for 60 min at 70 °C, and centrifuged at 6,000 rpm for 20 min. Then, the supernatant was collected by Whatman No. 1 filter paper.	flavones, polyphenols, and terpenoids	Rahaiee *et al.* (2020)
Golden apple	*Aegle marmelos*	2.974 g of Zn $(NO_3)_2{\cdot}6H_2O$ was added to 10 ml of the as-prepared juice taken in silica crucibles and dissolved to get homogenous solutions.		Anupama *et al.* (2018)
Guava	*Psidium guajava*	1 M zinc acetate precursor to 100 ml leaf extract	β-Carotene and meochrome	Saha *et al.* (2018)

Table 2 | Photocatalytic degradation of dyes by plant-based ZnO nanoparticles

Plant extract	Plant part	Dyes degraded	References
Passiflora foetida	Peels	Organic dye	Khan *et al.* (2021)
Phoenix dactylifera	Pulp waste	Degradation of hazardous dyes	Rambabu *et al.* (2021)
Gynostemma pentaphyllum	Leaves	Malachite green	Park *et al.* (2021)
Carissa edulis	Fruits	Congo red	Fowsiya *et al.* (2016)
Anisochilus carnosus	Leaves	Methylene blue	Anbuvannan *et al.* (2015)
Aspalathus linearis	Flower	Photoluminescence	Diallo *et al.* (2015)
Plectranthus amboinicus	Leaves	photocatalytic activity	Fu & Fu (2015)
Caralluma Fimbriata	Aerial part	Indigo carmine	Mishra *et al.* (2016)
Sedum alfredii	Shoots	2-CP	Wang *et al.* (2016)
Carya illinoinensis	Shells and kernels	Rhodamine B	Ahmad *et al.* (2021)
Olea europaea	Leaves	Degradation of environmental pollutants.	Hashemi *et al.* (2016)
Camellia sinensis	Leaves	Methylene blue, malachite green	Gonçalves *et al.* (2021)
Cyanometra ramiflora	Leaves	Rhodamine B	Varadavenkatesan *et al.* (2019)
Thymus vulgaris	Leaves	Methylene blue	Jaffri & Ahmad (2019)
Moringa oleifera	Leaves	Titan yellow	Pal *et al.* (2018)
Aloe barbadensis	Peel	Remove organic compounds	Lau *et al.* (2020)
Abelmoschus	Leaves	Methylene blue and Methyl orange	Mirgane *et al.* (2020)
Eucalyptus globulus	Leaves	Methylene blue and Methyl orange	Siripireddy & Mandal (2017)
Azadirachta indica	Leaves	Methylene blue	Fagier (2021)
Coriandrum sativum	Leaves	Yellow 186	Singh *et al.* (2019)
Quercus	Fruit hull	Basic violet 3	Sorbiun *et al.* (2018)
Garcinia mangostana	Fruit	Malachite green	Perera *et al.* (2020)
Mussaenda frondosa	Leaves/stem	Methylene blue	Jayappa *et al.* (2020)
Sambucus ebulus	Leaves	Methylene blue	Alamdari *et al.*(2020)
Vitex trifolia	Leaves	Methylene blue	Elumalai *et al.* (2015)
Brassica oleracea L. var. *italica*	Broccoli leaves	Methylene blue/Phenol red	Osuntokun *et al.* (2019)
Tabernaemontana divaricate	Leaves	Methylene blue	Raja *et al.* (2018)
Dolichos lablab	Leaves	Methylene blue/Rhodamine B (RhB), orange II (OII)	Kahsay *et al.* (2019)
Hippophae rhamnoides	Fruit	Malachite green/Congo red/Methylene blue /Eosin Y	Rupa *et al.* (2019)
Cannabis sativa	Leaves	Congo red/Methyl orange	Chauhan *et al.* (2020)
Euphorbia prolifera	Leaves	Methylene blue/Congo red	Momeni *et al.* (2016)
Piper betel	Leaves	Methylene blue	Rajesh *et al.* (2016)
Psidium guajava	Leaves	Methylene blue	Essawy (2018), Saha *et al.* (2018)
Ocimum basilicum	Leaves	Malachite green	Chijioke-Okere *et al.* (2019)
Hibiscus sabdariffa	Flower	Methylene blue	Soto-Robles *et al.* (2019)
Melia azedarach	Leaves	Azo dyes	Weldegebrieal (2020)
Scutellaria baicalensis	Root	Methylene blue	Chen *et al.* (2019)
Ziziphus jujuba	Fruit	Methylene blue and Eriochrome black-T	Golmohammadi *et al.* (2020)

(*Continued.*)

Table 2 | Continued

Plant extract	Plant part	Dyes degraded	References
Calliandra haematocephala	Leaves	Methylene blue	Vinayagam *et al.* (2020)
Trianthema portulacastrum	Leaves	Synozol Navy Blue-KBF textile	Khan *et al.* (2019)
Averrhoe carrambola	Fruit extract	Congo red	Chakraborty *et al.* (2020)
Tectona Grandis	Leaves	Methylene blue	Raizada *et al.* (2019)
Sageretia thea	Leaves	Crystal violet	Talha Khalil *et al.* (2019)
Abelmoschus esculentus	Leaves	Methylene blue and Methyl orange	Mirgane *et al.* (2020)
Nephelium lappaceum	Peel extract	Methyl orange	Karnan & Selvakumar (2016)
Kalopanax septemlobus	Bark extract	Methylene blue	Lu *et al.* (2019)
Cassia fistula	Plant extract	Methylene blue	Suresh *et al.* (2015)
Artocarpus heterophyllus	Leaves	Rose Bengal	Vidya *et al.* (2016)
S. lycopersicum	Leaves	Congo Red	Preethi *et al.* (2020)
Leucaena leucocephala	Leaves	Gentian violet, Crystal violet	Kanagamani *et al.* (2019)
Garcinia xanthochymus	Fruits	Methylene blue	Nethravathi *et al.* (2015)
Zingiber officinale	Root	Methylene blue	Haider *et al.* (2020)
Allium sativum	Root	Methylene blue	Haider *et al.* (2020)
Prunus cerasifera	Leaves	Bromocresol green, bromophenol blue, methyl red, and methyl blue	Jaffri & Ahmad (2019)
Aerva lanata	Flower	Rhodamine B	Duraimurugan *et al.* (2020)
Aerva javanica	Flower	Rhodamine B	Duraimurugan *et al.* (2020)
Panax ginseng	Flower	Methylene blue, Eosin Y, and Malachite green	Kaliraj *et al.* (2019)
Acanthopanax senticosus	Flower	Methylene blue, Eosin Y, and Malachite green	Kaliraj *et al.* (2019)
Kalopanax septemlobus	Flower	Methylene blue, Eosin Y, and Malachite green	Kaliraj *et al.* (2019)
Dendropanax morbifera	Flower	Methylene blue, Eosin Y, and Malachite green	Kaliraj *et al.* (2019)
Cocus nucifera	Water	Organic methylene blue	Satheshkumar *et al.* (2020)
Curry tree	Leaves	Organic methylene blue	Satheshkumar *et al.* (2020)
Rubus coreanus	Fruit	Malachite green	Rupa *et al.* (2018)
Vitex agnus-castus	Leaves	Methylene blue and Crystal violet	Dobrucka (2019)
Linum usitatissimum	Seeds	Methylene blue	Alkasir *et al.* (2020)
Cyadonia	Seeds	Methylene blue	Moghaddas *et al.* (2020)
Hydnocarpus alpina	Leaves	Methylene blue	Ganesh *et al.* (2019)
Ipomoea pes-caprae	Leaves	Methylene blue	Venkateasan *et al.* (2017)
Monsonia burkeana	Plant extract	Methylene blue	Ngoepe *et al.* (2018)
Allium cepa	Onion peels	Methylene blue and Crystal violet	Rajkumar *et al.* (2019)
Rheum turketanicum	Rhizome extract	Methylene blue	Nemati *et al.* (2019)
Petroselinum crispum	Leaves	Methylene blue	Stan *et al.* (2015)
	Seeds	Methylene blue	Shabaani *et al.* (2020)
Amomum longiligulare	Fruit extract	Methylene blue and Malachite green	Liu *et al.* (2020)
Suaeda japonica Makino	Plant extract	Methylene blue	Shim *et al.* (2019)
Crocus sativus	Leaves	Methylene blue	Rahaiee *et al.* (2020)
Aegle marmelos	Fruit pulp	Methylene blue	Anupama *et al.* (2018)
Corriandrum sativum	Leaves	Anthracene	Hassan *et al.* (2015)

Table 3 | Synthesis of ZnO nanoparticle from microorganisms

Microorganism species	Genus	Extraction method	Nanoparticle shape	Nanoparticle size	References
Algae					
Sargassum muticum	*Sargassum*	Dried algae powder (2 g) was mixed with 100 ml distilled water, heated to 100 °C, and filtered through Whatman No. 41 filter paper.	Hexagonal structures	42 nm	Azizi *et al.* (2014)
Cladophora glomerata	*Cladophora*	Algae samples were washed with distilled water to remove the adhering particles. They were dried in the shaded place. The dried algae were powdered.	Irregular shapes	14.39 nm to 37.85 nm	Abdulwahid *et al.* (2019)
Chlamydomonas reinhardtii	*Chlamydomonas*	25 mL of algal extract was made up to 100 mL using deionized water; zinc acetate dehydrate was added to obtain a final concentration of 1 mM.	Nanoflowers	40 nm	Parthasarathy & Narayanan (2014)
Gracilaria edulis	*Gracilaria*	Fresh alga (10 g) was mixed in 50 mL of sterile distilled water and chopped into fine pieces of approximately 1 mm. The mixture was then boiled by microwave oven irradiation for 10 min. Then, the extract was filtered through Whatman No. 1 filter paper.	Nanorods		Priyadharshini *et al.* (2014)
Bacteria					
Arthrospira platensis	*Arthrospira*	0.44 g of zinc nitrate was dissolved in 2 mL of distilled H_2O. The 98 mL of biomass filtrated was added to get a final concentration of 2 mM. The mixture was incubated for 24 h at 30 °C $\pm$2 °C and 150 rpm shaking conditions.	Spheres	30.0 to 55.0 nm	El-Belely *et al.* (2021)
Lactobacillus sporogenes	*Bacillus*	10 mL of culture was doubled in volume by mixing an equal volume of sterile distilled water containing nutrients in five different hard glass test tubes. 20 mL of zinc chloride solution was added and heated on the steam bath up to 80 °C for 5 to 10 minutes.	Hexagonal structures	11 nm	Prasad & Jha (2009)
Pseudomonas aeruginosa	*Pseudomonas*	The culture was centrifuged at 12,000 rpm for 15 min. The obtained supernatant was collected in the sterile separating funnel, acidified by 12 N HCl (pH 2.0) to precipitate, and incubated at 4 °C.	Spheres	35 to 80 nm	Singh *et al.* (2014)
Bacillus haynesii	*Bacillus*	100 mL of cell-free supernatant and 100 mL of zinc sulphate solution (1 mM) were taken, and the mixture was placed on a stirrer at room temperature for 24 h.	Rods	50 $\pm$ 5 nm	Rehman *et al.* (2019)
Bacillus licheniformis	*Bacillus*	Zinc acetate dihydrate was dissolved in 50 ml of deionized water in a flask and heated at 60 °C for 15 min followed by the addition of (0.6 M) sodium bicarbonate. Wet bacterial biomass (5 g) was then added to the mixture. The above solution was incubated under continuous stirring (200 rpm) for 48 h at 37 $\pm$ 1 °C.	Nano flower	300 nm	Tripathi *et al.* (2014)
Halomonas elongata	*Halomonas*	Taguchi method to obtain optimum conditions in zinc oxide nanoparticles (NPs) biosynthesis by *Halomonas elongata* IBRC-M 10214.	Spheres	18.11 $\pm$ 8.93 nm	Taran *et al.* (2018)
Aeromonas hydrophila	*Aeromonas*	The diluted culture solution was again allowed to grow for another 24 h. 20 mL of 0.1 g ZnO were added to the culture solution, and it	Spheres	57.72 nm	Jayaseelan *et al.* (2012)

		was kept under shaking incubator at 120 rpm at 30 °C for 24 h until white deposition starts to appear at the bottom of the flask, indicating the initiation of transformation.			
Bacillus sp.	*Bacillus*	The bacteria are mixed with alginate and used for experiments.	Beads	2 mm	Cai *et al.* (2020)
Fungus					
Pichia kudriavzevii	*Candida*	Fungal mycelia were separated from the culture medium through centrifugation and sterile water to remove any components of the medium. 20 g of biomass was resuspended in 100 mL of sterile deionized Milli-Q water.	Hexagonal and irregular shapes	10–61 nm	Moghaddam *et al.* (2017)
Periconium sp.	*Periconia*	20 g of zinc nitrate was dissolved in 100 ml of deionized water under constant stirring in a hot plate at 90 °C. 25 ml of fungal extract was added to the zinc nitrate solution, and the solution was evaporated to form a solution at pH 5, and it was kept as it is. The resultant sol was held in a hot air oven at 45 °C for 24 h.	hexagonal wurtzite	40 nm	Ganesan *et al.* (2020)
Phanerochaete chrysosporium	*Phanerochaete*	Fungal culture was inoculated in malt extract broth (150 ml) and incubated for 5–7 days, then filtered through Whatman filter paper No. 1 and added to zinc sulphate solution, followed by drop-wise addition of sodium hydroxide until the appearance of white suspended nanoparticles and again it was incubated for 24 h at 27 °C.		50 nm	Sharma *et al.* (2020)
Aspergillus terreus	*Aspergillus*	Fungal strains were taken to separate and purify the synthesized. The ultra-centrifugation collected NPs at 20,000 rpm (20 min), washed in deionized water with ethanol, and dried at 50 °C.	Spheres with irregular margins	30.45 nm	Mousa *et al.* (2021)
Cochliobolus geniculatus	*Cochliobolus*	10 g of fungal biomass was transferred to 100 ml of sterile ultrapure water and incubated for 72 h. The mycelial free filtrate was obtained by separating fungal mycelial biomass by centrifugation and combined with 1 mM of zinc acetate and maintained at 28 ± 1 °C for 72 h in an incubator shaker.	Spheres	2–6 nm	Kadam *et al.* (2019)
Marine yeast		The cultured broth was collected after incubation and centrifuged at 8,000 rpm for 15 minutes. The supernatant was added with 1 mm of ZnO.	Round	86.27 nm	Aswathy *et al.* (2017)
Trichoderma harzianum	*Trichoderma*	50 ml of aqueous culture in flasks by stirring with zinc nitrate was added in culture to make a final concentration of 1–2 mM solution. The reaction was carried out in dark conditions at 45 °C, stirring vigorously.	Spheres	87.5 nm	Consolo *et al.* (2020)
Penicillium chrysogenum	*Penicillium*	Fungal culture was grown up in a 100 mL fermentative broth medium for 7 days at pH 6.0, 30 °C, and shaking at 150 rpm, separated by Whatman filter paper No. 1.	Hexagonal and spherical structures	9.0–35.0 nm	Mohamed *et al.* (2020)

Table 4 | Photocatalytic degradation of dyes by microorganisms based ZnO nanoparticles

Microorganism species	Genus	Dye degraded	References
Algae			
Sargassum vulgare	*Sargassum*	Methylene blue	Karkhane *et al.* (2020)
Chlorella	*Chlorella*	Organosulfur pollutants	Khalafi *et al.* (2019)
Ulva lactuca	*Ulva*	Methylene blue	Zhu *et al.* (2019)
Chlamydomonas reinhardtii	*Chlamydomonas*	Methyl orange	Parthasarathy & Narayanan (2014)
Bacteria			
Arthrospira platensis	*Arthrospira*	Reactive red 120	Cardoso *et al.* (2012)
Pseudomonas putida and *Pseudomonas aureofaciens*	*Pseudomonas*	Textile effluent from Rajkot, Gujrat	Sur & Mukhopadhyay (2019)
Bacillus licheniformis	*Bacillus*	Methylene blue	Tripathi *et al.* (2014)
Bacillus sp.	*Bacillus*	Reactive blue 19	Cai *et al.* (2020)
Pseudochrobactrum sp.		Methanol blue and reactive black 5	Siddique *et al.* (2021)
Fungus			
Phanerochaete chrysosporium	*Phanerochaete*	Reactive Black 5 and Bismark Brown R	Kalpana *et al.* (2018)
Aspergillus niger	*Aspergillus*	Bismark brown	Enayatzamir *et al.* (2010)
Penicillium corylophilum	*Penicillium*	Methylene blue	Fouda *et al.* (2020)

brown) were studied on *Chlorella vulgaris,* which caused the inhibition of growth, pigment, and elemental composition of the cells. After exposure for 96 h, there was complete suppression of growth of algal cells, reduction in protein synthesis, and decrease in chlorophyll *a* pigment density (Gita *et al.* 2019).

MECHANISMS OF DYE REMOVAL USING ZnO NANOPARTICLES

There are different types of synthetic textile dyes which include azo dyes, basic dyes, acidic dyes, nitro dye, disperse dye, vat dyes, direct dyes, mordant dye, reactive dye, solvent dye, reactive and sulfur dyes. The photocatalytic degradation mechanism is the same for all synthetic dyes, but they differ in the degraded product released. The zinc nanoparticles synthesized using medicinal plants are the mechanism responsible for degradation of azo dyes with the help of biosynthesized ZnO NPs under sunlight and UV irradiation. ZnO is a photocatalyst that helps in the degradation of dyes present in wastewater. ZnO nanoparticles are cost-efficient, and highly photoactive in the UV region. The plant extracted nanoparticles affect the morphology, and concentration of oxygen vacancies. The involvement of phytochemicals in nanoparticle synthesis increases the efficiency of ZnO NPs (Weldegebrieal 2020). Recent studies however showed that neither visible LEDs nor UV C irradiation resulted in photocatalytic bisphenol-A degradation. The inability of the amalgam UV C lamp to promote photocatalytic reactions in the vertical position could be attributed to either spatial photon emission caused by mercury gas settlement or photon–nanoparticle interaction at an incorrect collision angle. The vertically positioned UV LED-based illumination system, however, achieved a high energy consumption efficiency. Bisphenol-A was removed in the same manner as in the horizontally positioned reactor configuration, although the energy efficiency was almost unchanged (Tunçal 2020).

ZnO nanoparticles were dispersed in an azo dye mixture in water in a ratio of 1:10 (w/v pH = 6) under sonication for 20 min. The mixture was irradiated by sunlight, and absorption can be measured at regular intervals to observe the degradation of dyes. When light passes through the solution, electron–hole pair generation takes place (Equations (1) and (2)). The oxidation and reduction process creates free radicals and superoxides (Equation (3)) (Fageria *et al.* 2014). The OH functional group present in nanoparticles interacts with dye particles to generate OH free radicals (Equation (4)). The detailed

Table 5 | List of azo dyes affecting water bodies

Dye Name	Dye iconicity	Toxicity	References
Acid red	Anionic	Carcinogen	Sudha *et al.* (2018)
Acid violet	Anionic	Chromosomal aberration, lipid peroxidation	Sudha *et al.* (2018)
Acid yellow	Anionic	Carcinogen	Swen *et al.* (2020)
Allura red	Anionic	Genotoxic *in vivo* in mice and rats, hypersensitivity	Kobylewski & Jacobson (2012)
Amaranath	Anionic	Allergy, tumor, congenital disabilities, respiratory Problems	Basu & Suresh Kumar (2014)
Aniline yellow	Nonionic	Carcinogen	Chung (2016)
Bismarck brown R	Nonionic	Carcinogen	Fatima *et al.* (2019)
Bismarck brown Y	Cationic	Carcinogen	Soriano *et al.* (2014)
Direct blue 6	Anionic	Carcinogen	Lazear *et al.* (1979)
Direct blue 15	Anionic	Carcinogen	Javaid & Qazi (2019)
Direct brown	Anionic	Carcinogen	Lazear *et al.* (1979)
Direct red 28	Anionic	Carcinogen	Shetti *et al.* (2019)
Direct orange	Anionic	Retards growth in plants	Ventura-camargo & Marin-morales (2013)
Disperse Orange 3	Nonionic	Allergic	Ventura-camargo & Marin-morales (2013)
Disperse blue	Cationic	Mutagenic, cytotoxic	Chequer *et al.* (2011)
Disperse red	Nonionic	Mutagenic	Kisku *et al.* (2015)
Disperse Yellow 3	Nonionic	Carcinogen	Kisku *et al.* (2015)
Methyl orange	Anionic	Mutagenic	Freeman *et al.* (1996)
Methyl yellow	Nonionic	Carcinogen	Chung (2016)
Reactive black 5	Anionic	Carcinogen	Sudha *et al.* (2018)
Reactive brilliant red	Anionic	Inhibits functioning of human serum albumen	Bafana *et al.* (2011)
Sudan I	Nonionic	Carcinogen	Stiborová *et al.* (2002)
Sudan II	Nonionic	Mutagen	Pan *et al.* (2012)
Sudan III	Nonionic	Carcinogen	Pietruk *et al.* (2019)
Sudan IV	Nonionic	Carcinogen	Pietruk *et al.* (2019)

mechanism of the photolytic dye degradation mechanism is shown below:

$$ZnO + \text{Light energy} \rightarrow h^{+} + e^{(-)} \quad (1)$$

$$e^{(-)} + O_2 \rightarrow O^{\cdot -2} \quad (2)$$

$$h^{+} + OH^{-} \rightarrow OH \quad (3)$$

$$O^{\cdot -2}/OH + \text{Dye solution}^{+} \rightarrow \text{Degradation products} + \text{by-products } (CO_2 + H_2O) \quad (4)$$

The azo dye solutions can be prepared by making a stock solution of the desired concentration. This dye mixture has varying concentrations of nanoparticles in normal pH and is exposed to light. The concentration reduction can be calculated using Equation (5):

$$\text{Degradation rate } (\%) = \frac{A_o - A}{A_o} \times 100 \quad (5)$$

In the equation, A_0 depicts the initial concentration of the dye solution, and A depicts the final concentration of the dye solution after the photocatalytic process (Fageria *et al.* 2014).

FACTORS AFFECTING DYE DEGRADATION

The degradation process can be affected by many factors, like size, pH, temperature, aeration, catalysts, dopants, and oxidation. The surface area plays an important role in catalysis reaction, and a bigger particle size inhibits the reaction (Talebian *et al.* 2013). The photodegradation observed in nano-size particles was more efficient than micro-size particles because of the high surface area and more availability of active sites (Ateeq 2012). The effect of pH on photodegradation was measured in the ranges 4, 7, and 10. The methyl orange dye was removed efficiently at pH = 7, and pollutants were efficiently removed at pH = 4 (Abbasi & Hasanpour 2017). ZnO at higher pH efficiently degrades anionic dyes such as Congo red. Photodegradation was better at pH = 10 than pH = 7 due to the high concentration of hydroxyl ions (Adam *et al.* 2018). The temperature varies for each dye to be degraded. The degradation of direct red-23 dye at different annealing temperatures showed different efficiencies of degradation, which include temperatures in the range of 400 °C, 500 °C, 700 °C, and 800 °C, and photodegradation efficiencies were 88.48%, 95.49%, 92.63%, and 86.40%, respectively. It was observed that at 600 °C annealing temperature, complete degradation was observed (Umar *et al.* 2015). The synthesis of ZnO in the low-temperature reaction was efficient in Congo red degradation (Ong *et al.* 2016). The Reactive green 19 dye showed 77% degradation under 7 h in the presence of aeration, but in the absence of aeration, it resulted in the extension of reaction time to 8 h and a decrease in degradation efficiency to 56% (Lee *et al.* 2017). The ZnO nanoparticles extracted from *Prosopis juliflora* leaf extract degraded methylene blue with an efficiency of 99% under UV illumination and continuous aeration (Sheik Mydeen *et al.* 2020). The efficiency of degradation was directly proportional to the catalyst concentration. The reaction could not be proceeded due to the low catalyst surface. The degradation efficiency of decomposing methyl orange gradually increased from 50, 200, and 1,000 nm ZnO photocatalysts at pH = 10 (Wang *et al.* 2007). With increased catalyst concentration, it opens up more active sites for interaction with the dye solution. The methylene blue degradation was higher at a high concentration of catalyst (de Moraes *et al.* 2018). The concentration of dopants was inversely proportional to degradation efficiency. Metals like Ni, Co, and Ti act as doping metals and affect degradation efficiency (Mohseni-Salehi *et al.* 2018). Silver-doped (2%) ZnO nanoparticles used to degrade Brilliant green dye resulted in higher photocatalytic efficiency than alone (Gnanaprakasam *et al.* 2016). The photolytic degradation of Brilliant green was 99% in the presence of TiO_2 (Munusamy *et al.* 2013). The photocatalytic degradation of Acid orange 7 dye follows first-order kinetics under the presence of hydrogen peroxide and sodium periodate (Sadik 2007). The degradation efficiency of dye decreased with an increase in dye concentration, and the rate increased with $C_{oxidant}/C_{dye}$ ratio (Madhavan *et al.* 2006). The behaviour of ZnO suspensions was investigated at pH values ranging from 3 to 11 in order to investigate pH variation, the effect of dissolution on the zeta potential, and aggregate size stability. For all three constituents, the most stable pH region achieved in 1 hour corresponds to an initial pH of 7.7 (Fatehah *et al.* 2014).

ADSORPTION

The adsorption of dyes is essential to the efficient degradation of dyes. Several workers suggested that there was no relationship between adsorption of dyes and degradation in which they have used both anionic and cationic dyes (Liu *et al.* 2013). However, ZnO nanospheres were prepared by using a hydrothermal method and used efficient azo dye (Bismarck brown) in which different parameters affected the adsorption of dye and degradation by ZnO (Zaidi *et al.* 2019). Malachite green, Alexa fluor, and Congo red adsorbed a maximum of 2,963, 3,307, and 1,554 mg/g, respectively, on ZnO nanoparticles. The temperature and pH play an essential role in the adsorption process. The adsorption process was maximized by chemical precipitation, electrostatic attraction, and hydrogen bonding between the ZnO nanoparticle and different dyes (Zhang *et al.* 2016). ZnO supported with activated carbon or brick grain particles using the simple co-precipitation method resulted in a higher adsorption capacity for Malachite green and Congo red dyes (Raizada *et al.* 2014).

THE COMBINED ACTION OF ADSORPTION AND PHOTOCATALYTIC ACTIVITY OF ZINC OXIDE NANOPARTICLES IN DYE DEGRADATION

Adsorption and photocatalytic activity of the ZnO nanoparticles showed a higher efficiency to degrade the dyes. ZnO/Ag-montmorillonite nanoparticles with *Urtica dioica* leaf extract increased the discoloration of methylene blue from 38.95 to

91.95% (Sohrabnezhad & Seifi 2016). ZnO–CuO thin films were prepared by carbothermal evaporation with ZnO and Cu, and photocatalysis of methyl orange and methylene blue was observed in visible and UV light (Kuriakose *et al.* 2015). ZnO–graphene nanocomposites using grape and *Eichhornia crassipes* leaf extract degraded Rhodamine B dye efficiently with 70.0% and 97.5% degradation rate (Ramanathan *et al.* 2019). ZnO nanospheres generated by the hydrothermal method followed the pseudo-first-order rate reaction, degraded Bismarck brown dye with an efficiency of 94% after 2 hours of exposure (Zaidi *et al.* 2019). ZnO-graphene obtained by the hydrothermal process degraded Azure B dye 99% within 20 minutes of exposure under UV illumination (Rabieh *et al.* 2016). *Strobilanthes crispus* (B.) leaf extract fabricated with La_2CuO_4-decorated ZnO were capable of degrading Malachite green dye following pseudo-first-order kinetics (Yulizar *et al.* 2020).

MITIGATION OF ZnO NANOPARTICLE TOXICITY

Zebrafish share 70% of their genes with human beings. ZnO nanoparticles damage neural and vascular systems. Dissolved Zn causes less damage to the nervous system than chemically synthesized ZnO particles. Zebrafish when exposed to dissolved oxygen matter (DOM) water with ZnO nanoparticles, it converted to zinc ions that are toxic. ZnO damages the hatching rates and degrades the DOM (Kteeba *et al.* 2018). The ZnO nanoparticles synthesized from plant extracts are more efficient and eco-friendlier than chemically synthesized nanoparticles. Plant extracts were used as a reducing and stabilizing agent, and zinc nitrate can be used as a zinc precursor. ZnO nanoparticles are exposed to sunlight and electrons become excited from the valence band to conduction band resulting in the formation of superoxides and hydrogen oxide radicals which are potent reducing agents that are capable of degrading dyes, resulting in a less toxic degradation products such as carbon dioxide and water (Sharma *et al.* 2021).

FATE AND TOXICITY OF ZINC OXIDE NANOPARTICLES

In today's world, we use nanoparticles in all fields that lead to the accumulation of ZnO nanoparticles. When nanoparticles reach the water bodies, it leads to aggregation of nanoparticles that in suspension form, converted to zinc ions that induce toxicity (Beegam *et al.* 2016). ZnO nanoparticles enter the soil, and are converted to Zn^{2+} in soil and plants. The soluble Zn was more toxic than ZnO nanoparticles (Wang *et al.* 2013).

ZnO nanoparticles affect soil, water bodies, the environment, and human health. Zn deficiency in humans leads to severe anemia, weakening of the immune system, inflammation, and lung toxicity due to inhalation of ZnO nanoparticles (Beegam *et al.* 2016; Rajput *et al.* 2018). The toxicity of ZnO nanoparticles can be observed in mammalian cells, bacteria, and zebrafish. In bronchial epithelial cell lines such as BEAS-2B and A549 cells, ZnO nanoparticles induce cytotoxicity and mitochondrial dysfunction. ZnO had both short-term and long-term effects on mammalian cells, and short-term effects included apoptosis, whereas long-term effects included increased ROS generation, and decreased mitochondrial activity (Vandebriel & De Jong 2012). The nanoparticles are toxic to both Gram-positive and Gram-negative bacteria as nanoparticles are bactericidal at the log phase of bacterial growth, and cell viability/membrane integrity was lost after 15 h of exposure. (Reddy *et al.* 2007). When ZnO nanoparticles enter the marine environment this leads to ROS production, toxicity in zebrafish embryos, and damage in their hatching enzyme due to hypoxia caused by ZnO nanoparticles (Bai *et al.* 2010) (Yung *et al.* 2014).

MECHANISM OF TOXICITY OF ZnO NANOPARTICLES IN *IN VITRO* MODELS

The highly toxic deposition of dyes in water bodies stops the oxygenation capacity of water and blocks sunlight from penetrating inside, affecting the biological activity of aquatic life and the photosynthesis process of aquatic plants. The dyes keep on accumulating in the sediments, in fishes, or other marine organisms. Decomposition of dyes into water bodies are carcinogenic or mutagenic compounds that cause allergies, skin irritation, or different tissue changes. The toxicity was observed in mammalian cells, which mimics human cell conditions in which briefly the authors have reported that ZnO induces cytotoxicity but not Zn^{2+}. To understand the mechanism, they performed *in vitro* studies on bronchial epithelial cell lines, dermal cell lines, colon cell lines, and immune cells (RAW264.7). The ZnO nanoparticles dissolved the extracellular membranes of the cells and were converted to Zn^{2+} that leads to lysosome destabilization. As zinc ion concentration increases inside the cells, it leads to a decrease in enzyme and transcription factors. Proteins such as bovine serum albumin adsorb to the surface of ZnO. ZnO damages the cells, which leads to calcium flux, ROS generation, membrane damage, and mitochondrial dysfunction (Vandebriel & De Jong 2012). Nanoparticles induce toxicity in both Gram-positive and Gram-negative bacteria

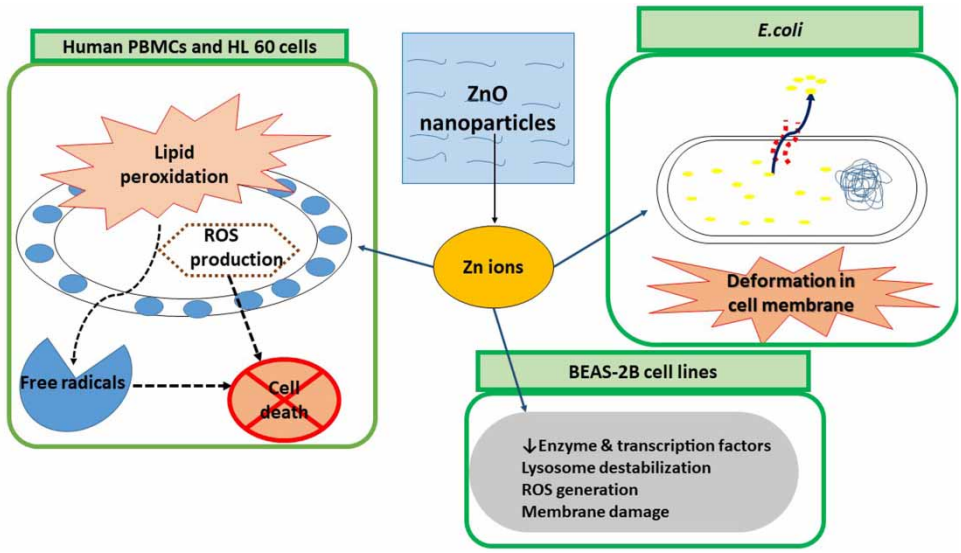

Figure 2 | Mechanism of toxicity due to ZnO nanoparticles.

and caused cell proliferation in cancer cells. The ultra-sonication of HL60 cancerous cell lines induced lipid peroxidation, which leads to enhancement of the mechanism in the presence of ZnO nanoparticles (Premanathan *et al.* 2011). *E. coli* is the most common pathogen that can be used to see toxicity mechanisms. The ZnO nanoparticles dissolve in medium and release Zn ions. High concentrations of ZnO nanoparticles damage physiological features, decreases toxicity tolerance levels, and causes deformation in the cell membrane, and leaking out of intercellular substances. The release of zinc ions leads to maximum toxicity (Li *et al.* 2011) (Figure 2).

CONCLUSION AND FUTURE OUTLOOK

Organic pollutants such as azo dyes are common environmental pollutants, and considered hazardous materials for human health. Photocatalytic activity plays a significant role in the degradation of organic derivatives by ZnO and nanoparticles. ZnO nanoparticles have high thermal conductivity that helps in the removal of azo dye pollutants. Researchers have efficiently degraded azo dyes using plant-based nanoparticles. The photocatalytic degradation is enhanced by electron–hole pair generation. The nanoparticles generated from plant extracts help to increase the efficiency of degradation of dyes. Recently, several investigations have shown that plant extract nanomaterials have highly improved the photocatalytic efficiency compared to nanoparticles alone. To make nanoparticles, an appropriate compound, and an exclusive photocatalyst, researchers have tried different phytochemical concentrations to optimize the size of particles and surface area. Research has been carried out on numerous kinds of plant extract on ZnO as a photocatalyst by several approaches and the application in photodegradation of organic pollutants. The mechanism of toxicity is understood because of the interaction between the ZnO nanoparticles and different surfaces like bacteria, aquatic animals, and human cells. The deposition of nanoparticles damages cells, resulting in oxidative stress and is lethal to the environment and living organisms. The exact mechanisms of toxicity have still not been explored. With these pollutants either dyes or nanoparticles accumulate in water bodies and animal systems and this could pose a severe threat to health, especially in developing countries where water is consumed without much analysis or testing. Hence future posts should address new challenges for the application of ZnO in various emerging fields as well as well the identification of effects of these pollutants at the DNA level and how mutagenic they can be. However, these ZnO nanoparticles have been approved by the US FDA and are generally recognized as safe (GRAS), these nanoparticles can have huge prospects in the future towards biomedical, agricultural, and environmental remediation fields.

DATA AVAILABILITY STATEMENT

All relevant data are included in the paper or its Supplementary Information.

REFERENCES

Abbasi, S. & Hasanpour, M. 2017 The effect of pH on the photocatalytic degradation of methyl orange using decorated ZnO nanoparticles with SnO_2 nanoparticles. *Journal of Materials Science: Materials in Electronics* **28** (2), 1307–1314.

Abdulwahid, K. E., Dwaish, A. S. & Dakhil, O. A. 2019 Green synthesis and characterization of zinc oxide nanoparticles from *Cladophora glomerata* and its antifungal activity against some fungal isolates. *Plant Archives* **19** (2), 3527–3532.

Adam, R. E., Pozina, G., Willander, M. & Nur, O. 2018 Synthesis of ZnO nanoparticles by co-precipitation method for solar driven photodegradation of Congo red dye at different pH. *Photonics and Nanostructures – Fundamentals and Applications* **32**, 11–18.

Agarwal, H., Venkat Kumar, S. & Rajeshkumar, S. 2017 A review on green synthesis of zinc oxide nanoparticles – an eco-friendly approach. *Resource-Efficient Technologies* **3** (4), 406–413.

Ahmad, M., Rehman, W., Khan, M. M., Qureshi, M. T., Gul, A., Haq, S., Ullah, R., Rab, A. & Menaa, F. 2021 Phytogenic fabrication of ZnO and gold decorated ZnO nanoparticles for photocatalytic degradation of Rhodamine B. *Journal of Environmental Chemical Engineering* **9** (1), 104725.

Alamdari, S., Sasani Ghamsari, M. S., Lee, C., Han, W., Park, H. H., Tafreshi, M. J., Afarideh, H. & Ara, M. H. M. 2020 Preparation and characterization of zinc oxide nanoparticles using leaf extract of *Sambucus ebulus*. *Applied Sciences* **10** (10), 3620.

Alkasir, M., Samadi, N., Sabouri, Z., Mardani, Z., Khatami, M. & Darroudi, M. 2020 Evaluation cytotoxicity effects of biosynthesized zinc oxide nanoparticles using aqueous *Linum Usitatissimum* extract and investigation of their photocatalytic activityackn. *Inorganic Chemistry Communications* **119**, 108066.

Anbuvannan, M., Ramesh, M., Viruthagiri, G., Shanmugam, N. & Kannadasan, N. 2015 *Anisochilus carnosus* leaf extract mediated synthesis of zinc oxide nanoparticles for antibacterial and photocatalytic activities. *Materials Science in Semiconductor Processing* **39**, 621–628.

Anupama, C., Kaphle, A., Udayabhanu & Nagaraju, G. 2018 *Aegle marmelos* assisted facile combustion synthesis of multifunctional ZnO nanoparticles: study of their photoluminescence, photo catalytic and antimicrobial activities. *Journal of Materials Science: Materials in Electronics* **29** (5), 4238–4249.

Aswathy, R., Gabylis, B., Anwesha, S. & Bhaskara Rao, K. V. 2017 Green synthesis and characterization of marine yeast-mediated silver and zinc oxide nanoparticles and assessment of their antioxidant activity. *Asian Journal of Pharmaceutical and Clinical Research* **10** (10), 235–240.

Ateeq, S. O. A. 2012 *Water Disinfection by Photo-Degradation of Microorganisms Using Natural Dye-Sensitized ZnO Catalyst Water Disinfection by Photo-Degradation of Microorganisms Using Natural Dye-Sensitized ZnO Catalyst. (Doctoral dissertation)*.

Azizi, S., Ahmad, M. B., Namvar, F. & Mohamad, R. 2014 Green biosynthesis and characterization of zinc oxide nanoparticles using brown marine macroalga *Sargassum muticum* aqueous extract. *Materials Letters* **116**, 275–277.

Bafana, A., Devi, S. S. & Chakrabarti, T. 2011 Azo dyes: past, present and the future. *Environmental Reviews* **19** (1), 350–370.

Bai, W., Zhang, Z., Tian, W., He, X., Ma, Y., Zhao, Y. & Chai, Z. 2010 Toxicity of zinc oxide nanoparticles to zebrafish embryo: a physicochemical study of toxicity mechanism. *Journal of Nanoparticle Research* **12** (5), 1645–1654.

Basu, A. & Suresh Kumar, G. 2014 Targeting proteins with toxic azo dyes: a microcalorimetric characterization of the interaction of the food colorant amaranth with serum proteins. *Journal of Agricultural and Food Chemistry* **62** (31), 7955–7962.

Beegam, A., Prasad, P., Jose, J., Oliveira, M., Costa, F. G., Soares, A. M. V. M., Gonçalves, P. P., Trindade, T., Kalarikkal, N., Thomas, S. & Pereira, M. d. L. 2016 Environmental fate of zinc oxide nanoparticles: risks and benefits. *Toxicology – New Aspects to This Scientific Conundrum* (Soloneski, S. & Larramendy, M. L., eds.), Intech, pp. 81–112.

Brame, J., Li, Q. & Alvarez, P. J. J. 2011 Nanotechnology-enabled water treatment and reuse: emerging opportunities and challenges for developing countries. *Trends in Food Science and Technology* **22** (11), 618–624.

Cai, J., Liu, J., Pan, A., Liu, J., Wang, Y., Liu, J., Sun, F., Lin, H., Chen, J. & Su, X. 2020 Effective decolorization of anthraquinone dye reactive blue 19 using immobilized *Bacillus* sp. JF4 isolated by resuscitation-promoting factor strategy. *Water Science and Technology* **81** (6), 1159–1169.

Cardoso, N. F., Lima, E. C., Royer, B., Bach, M. V., Dotto, G. L., Pinto, L. A. A. & Calvete, T. 2012 Comparison of *Spirulina platensis* microalgae and commercial activated carbon as adsorbents for the removal of Reactive Red 120 dye from aqueous effluents. *Journal of Hazardous Materials* **241–242**, 146–153.

Chakraborty, S., Farida, J. J., Simon, R., Kasthuri, S. & Mary, N. L. 2020 *Averrhoe carrambola* fruit extract assisted green synthesis of ZnO nanoparticles for the photodegradation of Congo red dye. *Surfaces and Interfaces* **19**, 100488.

Chaudhary, A., Kumar, N., Kumar, R. & Salar, R. K. 2019 Antimicrobial activity of zinc oxide nanoparticles synthesized from *Aloe vera* peel extract. *SN Applied Sciences* **1** (1), 1–9.

Chauhan, A., Verma, R., Kumari, S., Sharma, A., Shandilya, P., Li, X., Batoo, K. M., Imran, A., Kulshrestha, S. & Kumar, R. 2020 Photocatalytic dye degradation and antimicrobial activities of pure and Ag-doped ZnO using *Cannabis sativa* leaf extract. *Scientific Reports* **10** (1), 1–16.

Chen, L., Batjikh, I., Hurh, J., Han, Y., Huo, Y., Ali, H., Li, J. F., Rupa, E. J., Ahn, J. C., Mathiyalagan, R. & Yang, D. C. 2019 Green synthesis of zinc oxide nanoparticles from root extract of *Scutellaria baicalensis* and its photocatalytic degradation activity using methylene blue. *Optik* **184**, 324–329.

Chequer, F. M. D., Dorta, D. J. & Oliveira, D. P. D. 2011 Azo dyes and their metabolites: does the discharge of the azo dye into water bodies represent human and ecological risks? *Advances in Treating Textile Effluent* **48**, 28–48.

Chijioke-Okere, M. O., Okorocha, N. J., Anukam, B. N. & Oguzie, E. E. 2019 Photocatalytic degradation of a basic dye using zinc oxide nanocatalyst. *International Letters of Chemistry, Physics and Astronomy* **81**, 18–26.

Chung, K.-T. 2016 Azo dyes and human health: a review. *Environmental Science Health Care* **34** (4), 1–60.

Consolo, V. F., Torres-Nicolini, A. & Alvarez, V. A. 2020 Mycosinthetized Ag, CuO and ZnO nanoparticles from a promising *Trichoderma harzianum* strain and their antifungal potential against important phytopathogens. *Scientific Reports* **10** (1), 1–9.

Dahiru, D., Onubiyi, J. A. & Umaru, H. A. 2006 Phytochemical screening and antiulcerogenic effect of *Moringa oleifera* aqueous leaf extract. *African Journal of Traditional, Complementary and Alternative Medicines* **3** (3), 70–75.

de Moraes, N. P., Silva, F. N., da Silva, M. L. C. P., Campos, T. M. B., Thim, G. P. & Rodrigues, L. A. 2018 Methylene blue photodegradation employing hexagonal prism-shaped niobium oxide as heterogeneous catalyst: effect of catalyst dosage, dye concentration, and radiation source. *Materials Chemistry and Physics* **214**, 95–106.

Diallo, A., Ngom, B. D., Park, E. & Maaza, M. 2015 Green synthesis of ZnO nanoparticles by aspalathus linearis: structural and optical properties. *Journal of Alloys and Compounds* **646**, 425–430.

Djurišić, A. B. & Leung, Y. H. 2006 Optical properties of ZnO nanostructures. *Small* **2** (8–9), 944–961.

Dobrucka, R. 2019 Facile synthesis of trimetallic nanoparticles Au/CuO/ZnO using *Vitex agnus-castus* extract and their activity in degradation of organic dyes. *International Journal of Environmental Analytical Chemistry* **00** (00), 1–12.

Duraimurugan, J., Suresh Kumar, G., Shanavas, S., Ramesh, R., Acevedo, R., Anbarasan, P. M. & Maadeswaran, P. 2020 Hydrothermal assisted phytofabrication of zinc oxide nanoparticles with different nanoscale characteristics for the photocatalytic degradation of Rhodamine B. *Optik* **202**, 163607.

El-Belely, E. F., Farag, M. M. S., Said, H. A., Amin, A. S., Azab, E., Gobouri, A. A. & Fouda, A. 2021 Green synthesis of zinc oxide nanoparticles (ZnO-NPs) using *Arthrospira platensis* (class: *Cyanophyceae*) and evaluation of their biomedical activities. *Nanomaterials* **11** (1), 1–18.

Elumalai, K., Velmurugan, S., Ravi, S., Kathiravan, V. & Adaikala Raj, G. 2015 Bio-approach: Plant mediated synthesis of ZnO nanoparticles and their catalytic reduction of methylene blue and antimicrobial activity. *Advanced Powder Technology* **26** (6), 1639–1651.

Enayatzamir, K., Alikhani, H. A., Yakhchali, B., Tabandeh, F. & Rodríguez-Couto, S. 2010 Decolouration of azo dyes by *Phanerochaete chrysosporium* immobilised into alginate beads. *Environmental Science and Pollution Research* **17** (1), 145–153.

Essawy, A. A. 2018 Silver imprinted zinc oxide nanoparticles: green synthetic approach, characterization and efficient sunlight-induced photocatalytic water detoxification. *Journal of Cleaner Production* **183**, 1011–1020.

Fageria, P., Gangopadhyay, S. & Pande, S. 2014 Synthesis of ZnO/Au and ZnO/Ag nanoparticles and their photocatalytic application using UV and visible light. *RSC Advances* **4** (48), 24962–24972.

Fagier, M. A. 2021 Plant-mediated biosynthesis and photocatalysis activities of zinc oxide nanoparticles: a prospect towards dyes mineralization. *Journal of Nanotechnology* **2021**, 6629180.

Fatehah, M. O., Aziz, H. A. & Stoll, S. 2014 Stability of ZnO nanoparticles in solution. Influence of pH, dissolution, aggregation and disaggregation effects. *Journal of Colloid Science and Biotechnology* **3**, 75–84.

Fathiazad, F., Matlobi, A., Khorrami, A., Hamedeyazdan, S., Soraya, H., Hammami, M., Maleki-Dizaji, N. & Garjani, A. 2012 Phytochemical screening and evaluation of cardioprotective activity of ethanolic extract of *Ocimum basilicum* L. (basil) against isoproterenol induced myocardial infarction in rats. *DARU. Journal of Pharmaceutical Sciences* **20** (1), 1–10.

Fatima, B., Siddiqui, S. I., Ahmed, R. & Chaudhry, S. A. 2019 Green synthesis of f-$CdWO_4$ for photocatalytic degradation and adsorptive removal of Bismarck Brown R dye from water. *Water Resources and Industry* **22**, 100119.

Feng, X. Y., Wang, Z., Zhang, C. W. & Wang, P. J. 2013 Electronic structure and energy band of IIIA doped group ZnO nanosheets. *Journal of Nanomaterials* **2013**, 1–6.

Fouda, A., Salem, S. S., Wassel, A. R., Hamza, M. F. & Shaheen, T. I. 2020 Optimization of green biosynthesized visible light active CuO/ZnO nano-photocatalysts for the degradation of organic methylene blue dye. *Heliyon* **6** (9), e04896.

Fowsiya, J., Madhumitha, G., Al-Dhabi, N. A. & Arasu, M. V. 2016 Photocatalytic degradation of Congo red using *Carissa edulis* extract capped zinc oxide nanoparticles. *Journal of Photochemistry and Photobiology B: Biology* **162**, 395–401.

Freeman, H. S., Hinks, D. & Esancy, J. 1996 Genotoxicity of azo dyes: bases and implications. *Physico-chemical Principles of Color* Chemistry, Chapman & Hall, Scotland, UK, pp. 254–292.

Fu, L. & Fu, Z. 2015 *Plectranthus amboinicus* leaf extract-assisted biosynthesis of ZnO nanoparticles and their photocatalytic activity. *Ceramics International* **41** (2), 2492–2496.

Ganesan, V., Hariram, M., Vivekanandhan, S. & Muthuramkumar, S. 2020 *Periconium* sp. (endophytic fungi) extract mediated sol-gel synthesis of ZnO nanoparticles for antimicrobial and antioxidant applications. *Materials Science in Semiconductor Processing* **105**, 104739.

Ganesh, M., Lee, S. G., Jayaprakash, J., Mohankumar, M. & Jang, H. T. 2019 *Hydnocarpus alpina* Wt extract mediated green synthesis of ZnO nanoparticle and screening of its antimicrobial, free radical scavenging, and photocatalytic activity. *Biocatalysis and Agricultural Biotechnology* **19**, 101129.

Garcia, M. A., Merino, J. M., Pinel, E. F., Quesada, A., De La Venta, J., González, M. L. R., Castro, G. R., Crespo, P., Llopis, J., González-Calbet, J. M. & Hernando, A. 2007 Magnetic properties of ZnO nanoparticles. *Nano Letters* **7** (6), 1489–1494.

Gita, S., Shukla, S. P., Saharan, N., Prakash, C. & Deshmukhe, G. 2019 Toxic effects of selected textile dyes on elemental composition, photosynthetic pigments, protein content and growth of a freshwater chlorophycean alga *Chlorella vulgaris*. *Bulletin of Environmental Contamination and Toxicology* **102** (6), 795–801.

Gnanaprakasam, A., Sivakumar, V. M. & Thirumarimurugan, M. 2016 A study on Cu and Ag doped ZnO nanoparticles for the photocatalytic degradation of brilliant green dye: synthesis and characterization. *Water Science and Technology* **74** (6), 1426–1435.

Golmohammadi, M., Honarmand, M. & Ghanbari, S. 2020 A green approach to synthesis of ZnO nanoparticles using jujube fruit extract and their application in photocatalytic degradation of organic dyes. *Spectrochimica Acta – Part A: Molecular and Biomolecular Spectroscopy* **229**, 117961.

Gonçalves, R. A., Toledo, R. P., Joshi, N. & Berengue, O. M. 2021 Green synthesis and applications of ZnO and TiO_2 nanostructures. *Molecules* **26** (8), 2236.

Güngördü, A., Birhanli, A. & Ozmen, M. 2013 Biochemical response to exposure to six textile dyes in early developmental stages of *Xenopus laevis*. *Environmental Science and Pollution Research* **20** (1), 452–460.

Haider, A., Ijaz, M., Imran, M., Naz, M., Majeed, H., Khan, J. A., Ali, M. M. & Ikram, M. 2020 Enhanced bactericidal action and dye degradation of spicy roots' extract-incorporated fine-tuned metal oxide nanoparticles. *Applied Nanoscience (Switzerland)* **10** (4), 1095–1104.

Hashemi, S., Asrar, Z., Pourseyedi, S. & Nadernejad, N. 2016 Green synthesis of ZnO nanoparticles by olive (*Olea europaea*). *IET Nanobiotechnology* **10** (6), 400–404.

Hassan, S. S. M., Azab, W. I. M. E., Ali, H. R. & Mansour, M. S. M. 2015 Green synthesis and characterization of ZnO nanoparticles for photocatalytic degradation of anthracene. *Advances in Natural Sciences: Nanoscience and Nanotechnology* **6** (4), 045012.

Hong, R. Y., Li, J. H., Chen, L. L., Liu, D. Q., Li, H. Z., Zheng, Y. & Ding, J. 2009 Synthesis, surface modification and photocatalytic property of ZnO nanoparticles. *Powder Technology* **189** (3), 426–432.

Jaffri, S. B. & Ahmad, K. S. 2019 Neoteric environmental detoxification of organic pollutants and pathogenic microbes via green synthesized ZnO nanoparticles. *Environmental Technology (United Kingdom)* **40** (28), 3745–3761.

Jain, S., Jain, A., Jain, N., Jain, D. K. & Balekar, N. 2010 Phytochemical investigation and evaluation of in vitro free radical scavenging activity of *Tabernaemontana divaricata* Linn. *Natural Product Research* **24** (3), 300–304.

Jain, K., Patel, A. S., Pardhi, V. P. & Flora, S. J. S. 2021 Nanotechnology in wastewater management: a new paradigm towards wastewater treatment. *Molecules (Basel, Switzerland)* **26** (6), 1797.

Javaid, R. & Qazi, U. Y. 2019 Catalytic oxidation process for the degradation of synthetic dyes: an overview. *International Journal of Environmental Research and Public Health* **16** (11), 1–27.

Jayappa, M. D., Ramaiah, C. K., Kumar, M. A. P., Suresh, D., Prabhu, A., Devasya, R. P. & Sheikh, S. 2020 Green synthesis of zinc oxide nanoparticles from the leaf, stem and *in vitro* grown callus of *Mussaenda frondosa LL.*: characterization and their applications. *Applied Nanoscience (Switzerland)* **10** (8), 3057–3074.

Jayaseelan, C., Rahuman, A. A., Kirthi, A. V., Marimuthu, S., Santhoshkumar, T., Bagavan, A., Gaurav, K., Karthik, L. & Rao, K. V. B. 2012 Novel microbial route to synthesize ZnO nanoparticles using *Aeromonas hydrophila* and their activity against pathogenic bacteria and fungi. *Spectrochimica Acta – Part A: Molecular and Biomolecular Spectroscopy* **90**, 78–84.

Kadam, V. V., Ettiyappan, J. P. & Mohan Balakrishnan, R. 2019 Mechanistic insight into the endophytic fungus mediated synthesis of protein capped ZnO nanoparticles. *Materials Science and Engineering B: Solid-State Materials for Advanced Technology* **243**, 214–221.

Kahsay, M. H., Tadesse, A., Ramadevi, D., Belachew, N. & Basavaiah, K. 2019 Green synthesis of zinc oxide nanostructures and investigation of their photocatalytic and bactericidal applications. *RSC Advances* **9** (63), 36967–36981.

Kaliraj, L., Ahn, J. C., Rupa, E. J., Abid, S., Lu, J. & Yang, D. C. 2019 Synthesis of panos extract mediated ZnO nano-flowers as photocatalyst for industrial dye degradation by UV illumination. *Journal of Photochemistry and Photobiology B: Biology* **199**, 111588.

Kalpana, V. N., Kataru, B. A. S., Sravani, N., Vigneshwari, T., Panneerselvam, A. & Devi Rajeswari, V. 2018 Biosynthesis of zinc oxide nanoparticles using culture filtrates of *Aspergillus niger*: antimicrobial textiles and dye degradation studies. *OpenNano* **3**, 48–55.

Kanagamani, K., Muthukrishnan, P., Saravanakumar, K., Shankar, K. & Kathiresan, A. 2019 Photocatalytic degradation of environmental perilous gentian violet dye using *Leucaena*-mediated zinc oxide nanoparticle and its anticancer activity. *Rare Metals* **38** (4), 277–286.

Karkhane, M., Lashgarian, H. E., Mirzaei, S. Z., Ghaffarizadeh, A., Cherghipour, K., Sepahvand, A. & Marzban, A. 2020 Antifungal, antioxidant and photocatalytic activities of zinc nanoparticles synthesized by *Sargassum vulgare* extract. *Biocatalysis and Agricultural Biotechnology* **29**, 101791.

Karnan, T. & Selvakumar, S. A. S. 2016 Biosynthesis of ZnO nanoparticles using rambutan (*Nephelium lappaceum* L.) peel extract and their photocatalytic activity on methyl orange dye. *Journal of Molecular Structure* **1125**, 358–365.

Khalafi, T., Buazar, F. & Ghanemi, K. 2019 Phycosynthesis and enhanced photocatalytic activity of zinc oxide nanoparticles toward organosulfur pollutants. *Scientific Reports* **9** (1), 1–10.

Khan, Z. U. H., Sadiq, H. M., Shah, N. S., Khan, A. U., Muhammad, N., Hassan, S. U., Tahir, K., Safi, S. Z., Khan, F. U., Imran, M., Ahmad, N., Ullah, F., Ahmad, A., Sayed, M., Khalid, M. S., Qaisrani, S. A., Ali, M. & Zakir, A. 2019 Greener synthesis of zinc oxide nanoparticles using *Trianthema portulacastrum* extract and evaluation of its photocatalytic and biological applications. *Journal of Photochemistry and Photobiology B: Biology* **192**, 147–157.

Khan, M., Ware, P. & Shimpi, N. 2021 Synthesis of ZnO nanoparticles using peels of *Passiflora foetida* and study of its activity as an efficient catalyst for the degradation of hazardous organic dye. *SN Applied Sciences* **3** (5), 1–17.

Khanna, P., Kaur, A. & Goyal, D. 2019 Algae-based metallic nanoparticles: synthesis, characterization and applications. *Journal of Microbiological Methods* **163**, 105656.

Kisku, G. C., Markandeya, Shukla, S. P., Singh, D. S. & Murthy, R. C. 2015 Characterization & adsorptive capacity of coal fly ash from aqueous solutions of disperse blue and disperse orange dyes. *Environmental Earth Sciences* **74** (2), 1125–1135.

Kobylewski, S. & Jacobson, M. F. 2012 Toxicology of food dyes. *International Journal of Occupational and Environmental Health* **18** (3), 220–246.

Köktürk, M., Altindağ, F., Ozhan, G., Çalimli, M. H. & Nas, M. S. 2021 Textile dyes maxilon blue 5G and reactive blue 203 induce acute toxicity and DNA damage during embryonic development of *Danio rerio*. *Comparative Biochemistry and Physiology Part – C: Toxicology and Pharmacology* **242**, 108947.

Kteeba, S. M., El-Ghobashy, A. E., El-Adawi, H. I., El-Rayis, O. A., Sreevidya, V. S., Guo, L. & Svoboda, K. R. 2018 Exposure to ZnO nanoparticles alters neuronal and vascular development in zebrafish: acute and transgenerational effects mitigated with dissolved organic matter. *Environmental Pollution* **242**, 433–448.

Kuriakose, S., Avasthi, D. K. & Mohapatra, S. 2015 Effects of swift heavy ion irradiation on structural, optical and photocatalytic properties of ZnO-CuO nanocomposites prepared by carbothermal evaporation method. *Beilstein Journal of Nanotechnology* **6** (1), 928–937.

Kurmukov, A. G. 2013 Phytochemistry of medicinal plants. *Medicinal Plants of Central Asia: Uzbekistan and Kyrgyzstan* **1** (6), 13–14.

Lau, G. E., Abdullah, C. A. C., Ahmad, W. A. N. W., Assaw, S. & Zheng, A. L. T. 2020 Eco-friendly photocatalysts for degradation of dyes. *Catalysts* **10** (10), 1–16.

Lazear, E. J., Shaddock, J. G., Barren, P. R. & Louie, S. C. 1979 The mutagenicity of some of the proposed metabolites of direct black 38 and pigment yellow 12 in the *Salmonella typhimurium* assay system. *Toxicology Letters* **4** (6), 519–525.

Lee, S. L., Ho, L. N., Ong, S. A., Wong, Y. S., Voon, C. H., Khalik, W. F., Yusoff, N. A. & Nordin, N. 2017 A highly efficient immobilized ZnO/Zn photoanode for degradation of azo dye reactive green 19 in a photocatalytic fuel cell. *Chemosphere* **166**, 118–125.

Lellis, B., Fávaro-Polonio, C. Z., Pamphile, J. A. & Polonio, J. C. 2019 Effects of textile dyes on health and the environment and bioremediation potential of living organisms. *Biotechnology Research and Innovation* **3** (2), 275–290.

Li, M., Zhu, L. & Lin, D. 2011 Toxicity of ZnO nanoparticles to *Escherichia coli*: mechanism and the influence of medium components. *Environmental Science and Technology* **45** (5), 1977–1983.

Liu, F., Leung, Y. H., Djurišić, A. B., Ng, A. M. C. & Chan, W. K. 2013 Native defects in ZnO: effect on dye adsorption and photocatalytic degradation. *Journal of Physical Chemistry C* **117** (23), 12218–12228.

Liu, Y. C., Li, J. F., Ahn, J. C., Pu, J. Y., Rupa, E. J., Huo, Y. & Yang, D. C. 2020 Biosynthesis of zinc oxide nanoparticles by one-pot green synthesis using fruit extract of *Amomum longiligulare* and its activity as a photocatalyst. *Optik* **218**, 165245.

Lu, J., Batjikh, I., Hurh, J., Han, Y., Ali, H., Mathiyalagan, R., Ling, C., Ahn, J. C. & Yang, D. C. 2019 Photocatalytic degradation of methylene blue using biosynthesized zinc oxide nanoparticles from bark extract of *Kalopanax septemlobus*. *Optik* **182**, 980–985.

Madhavan, J., Muthuraaman, B., Murugesan, S., Anandan, S. & Maruthamuthu, P. 2006 Peroxomonosulphate, an efficient oxidant for the photocatalysed degradation of a textile dye, acid red 88. *Solar Energy Materials and Solar Cells* **90** (13), 1875–1887.

Madhushika, H. G., Ariyadasa, T. U. & Gunawardena, S. H. P. 2020 Biological decolourization of textile industry wastewater by a developed bacterial consortium. *Water Science and Technology* **80** (10), 1910–1918.

Mirgane, N. A., Shivankar, V. S., Kotwal, S. B., Wadhawa, G. C. & Sonawale, M. C. 2020 Degradation of dyes using biologically synthesized zinc oxide nanoparticles. *Materials Today: Proceedings* **37** (Part 2), 849–853.

Mishra, P., Singh, Y. P., Nagaswarupa, H. P., Sharma, S. C., Vidya, Y. S., Prashantha, S. C., Nagabhushana, H., Anantharaju, K. S., Sharma, S. & Renuka, L. 2016 *Caralluma fimbriata* extract induced green synthesis, structural, optical and photocatalytic properties of ZnO nanostructure modified with Gd. *Journal of Alloys and Compounds* **685**, 656–669.

Moghaddam, A. B., Moniri, M., Azizi, S., Rahim, R. A., Ariff, A. B., Saad, W. Z., Namvar, F., Navaderi, M. & Mohamad, R. 2017 Biosynthesis of ZnO nanoparticles by a new *Pichia kudriavzevii* yeast strain and evaluation of their antimicrobial and antioxidant activities. *Molecules* **22** (6), 872.

Moghaddas, S. M. T. H., Elahi, B. & Javanbakht, V. 2020 Biosynthesis of pure zinc oxide nanoparticles using quince seed mucilage for photocatalytic dye degradation. *Journal of Alloys and Compounds* **821**, 153519.

Mohamed, A. A., Abu-Elghait, M., Ahmed, N. E. & Salem, S. S. 2020 Correction to: eco-friendly mycogenic synthesis of ZnO and CuO nanoparticles for *in vitro* antibacterial, antibiofilm and antifungal applications. *Biological Trace Element Research* **199**, 2800–2801.

Mohseni-Salehi, M. S., Taheri-Nassaj, E. & Hosseini-Zori, M. 2018 Effect of dopant (Co, Ni) concentration and hydroxyapatite compositing on photocatalytic activity of titania towards dye degradation. *Journal of Photochemistry and Photobiology A: Chemistry* **356**, 57–70.

Momeni, S. S., Nasrollahzadeh, M. & Rustaiyan, A. 2016 Green synthesis of the Cu/ZnO nanoparticles mediated by *Euphorbia prolifera* leaf extract and investigation of their catalytic activity. *Journal of Colloid and Interface Science* **472**, 173–179.

Mousa, S. A., El-Sayed, E. S. R., Mohamed, S. S., Abo El-Seoud, M. A., Elmehlawy, A. A. & Abdou, D. A. M. 2021 Novel mycosynthesis of Co_3O_4, CuO, Fe_3O_4, NiO, and ZnO nanoparticles by the endophytic *Aspergillus terreus* and evaluation of their antioxidant and antimicrobial activities. *Applied Microbiology and Biotechnology* **105** (2), 741–753.

Munusamy, S., Aparna, R. s. l. & Prasad, R. G. S. V. 2013 Photocatalytic effect of TiO2 and the effect of dopants on degradation of brilliant green. *Sustainable Chemical Processes* **1** (1), 4.

Nair, M. G., Nirmala, M., Rekha, K. & Anukaliani, A. 2011 Structural, optical, photo catalytic and antibacterial activity of ZnO and Co doped ZnO nanoparticles. *Materials Letters* **65** (12), 1797–1800.

Nemati, S., Hosseini, H. A., Hashemzadeh, A., Mohajeri, M., Sabouri, Z., Darroudi, M. & Oskuee, R. K. 2019 Cytotoxicity and photocatalytic applications of biosynthesized ZnO nanoparticles by *Rheum turketanicum* rhizome extract. *Materials Research Express* **6** (12), 125016.

Nethravathi, P. C., Shruthi, G. S., Suresh, D., Udayabhanu, Nagabhushana, H. & Sharma, S. C. 2015 *Garcinia xanthochymus* mediated green synthesis of ZnO nanoparticles: photoluminescence, photocatalytic and antioxidant activity studies. *Ceramics International* **41** (7), 8680–8687.

Ngoepe, N. M., Mbita, Z., Mathipa, M., Mketo, N., Ntsendwana, B. & Hintsho-Mbita, N. C. 2018 Biogenic synthesis of ZnO nanoparticles using *Monsonia burkeana* for use in photocatalytic, antibacterial and anticancer applications. *Ceramics International* **44** (14), 16999–17006.

Nikravesh, B., Shomalnasab, A., Nayyer, A., Aghababaei, N., Zarebi, R. & Ghanbari, F. 2020 UV/chlorine process for dye degradation in aqueous solution: mechanism, affecting factors and toxicity evaluation for textile wastewater. *Journal of Environmental Chemical Engineering* **8**, 5.

Ong, C. B., Mohammad, A. W., Rohani, R., Ba-Abbad, M. M. & Hairom, N. H. H. 2016 Solar photocatalytic degradation of hazardous Congo red using low-temperature synthesis of zinc oxide nanoparticles. *Process Safety and Environmental Protection* **104**, 549–557.

Osuntokun, J., Onwudiwe, D. C. & Ebenso, E. E. 2019 Green synthesis of ZnO nanoparticles using aqueous *Brassica oleracea* L. var. *italica* and the photocatalytic activity. *Green Chemistry Letters and Reviews* **12** (4), 444–457.

Özgür, Ü., Alivov, Y. I., Liu, C., Teke, A., Reshchikov, M. A., Doğan, S., Avrutin, V., Cho, S. J. & Morko¸, H. 2005 A comprehensive review of ZnO materials and devices. *Journal of Applied Physics* **98** (4), 1–103.

Packialakshmi, N. & Naziya, S. 2014 Screening of antibacterial and phytochemical analysis of *Caralluma fimbriata*. *The Pharma Innovation Journal* **3** (6), 65–69.

Pal, S., Mondal, S., Maity, J. & Mukherjee, R. 2018 Synthesis and characterization of ZnO nanoparticles using *Moringa oleifera* leaf extract: investigation of photocatalytic and antibacterial activity. *International Journal of Nanoscience and Nanotechnology* **14** (2), 111–119.

Pan, H., Feng, J., He, G. X., Cerniglia, C. E. & Chen, H. 2012 Evaluation of impact of exposure of Sudan azo dyes and their metabolites on human intestinal bacteria. *Anaerobe* **18** (4), 445–453. http://dx.doi.org/10.1016/j.anaerobe.2012.05.002.

Pappachen, L. K. & Sreelakshmi, K. S. 2017 Phytochemical screening and in vitro cytotoxicity studies of *Mussaenda frondosa* Linn leaves. *Research Journal of Pharmacy and Technology* **10** (12), 4227–4230.

Park, J. K., Rupa, E. J., Arif, M. H., Li, J. F., Anandapadmanaban, G., Kang, J. P., Kim, M., Ahn, J. C., Akter, R., Yang, D. C. & Kang, S. C. 2021 Synthesis of zinc oxide nanoparticles from *Gynostemma pentaphyllum* extracts and assessment of photocatalytic properties through malachite green dye decolorization under UV illumination-a green approach. *Optik* **239**, 166249.

Parthasarathy, P. & Narayanan, S. K. 2014 Effect of hydrothermal carbonization reaction parameters on. *Environmental Progress & Sustainable Energy* **33** (3), 676–680.

Perera, K. M. K. G., Kuruppu, K. A. S. S., Chamara, A. M. R. & Thiripuranathar, G. 2020 Characterization of spherical Ag nanoparticles synthesized from the agricultural wastes of *Garcinia mangostana* and *Nephelium lappaceum* and their applications as a photo catalyzer and fluorescence quencher. *SN Applied Sciences* **2** (12), 1–24.

Pietruk, K., Piątkowska, M. & Olejnik, M. 2019 Electrochemical reduction of azo dyes mimicking their biotransformation to more toxic products. *Journal of Veterinary Research (Poland* **63** (3), 433–438.

Prasad, K. & Jha, A. K. 2009 ZnO nanoparticles: synthesis and adsorption study. *Natural Science* **01** (02), 129–135.

Preethi, S., Abarna, K., Nithyasri, M., Kishore, P., Deepika, K., Ranjithkumar, R., Bhuvaneshwari, V. & Bharathi, D. 2020 Synthesis and characterization of chitosan/zinc oxide nanocomposite for antibacterial activity onto cotton fabrics and dye degradation applications. *International Journal of Biological Macromolecules* **164**, 2779–2787.

Premanathan, M., Karthikeyan, K., Jeyasubramanian, K. & Manivannan, G. 2011 Selective toxicity of ZnO nanoparticles toward Gram-positive bacteria and cancer cells by apoptosis through lipid peroxidation. *Nanomedicine: Nanotechnology, Biology, and Medicine* **7** (2), 184–192.

Priyadharshini, R. I., Prasannaraj, G., Geetha, N. & Venkatachalam, P. 2014 Microwave-mediated extracellular synthesis of metallic silver and zinc oxide nanoparticles using macro-algae (*Gracilaria edulis*) extracts and its anticancer activity against human PC3 cell lines. *Applied Biochemistry and Biotechnology* **174** (8), 2777–2790.

Rabieh, S., Nassimi, K. & Bagheri, M. 2016 Synthesis of hierarchical ZnO-reduced graphene oxide nanocomposites with enhanced adsorption-photocatalytic performance. *Materials Letters* **162**, 28–31.

Rahaiee, S., Ranjbar, M., Azizi, H., Govahi, M. & Zare, M. 2020 Green synthesis, characterization, and biological activities of saffron leaf extract-mediated zinc oxide nanoparticles: a sustainable approach to reuse an agricultural waste. *Applied Organometallic Chemistry* **34** (8), 1–12.

Raizada, P., Sudhaik, A. & Singh, P. 2019 Photocatalytic water decontamination using graphene and ZnO coupled photocatalysts: a review. *Materials Science for Energy Technologies* **2** (3), 509–525.

Raizada, P., Singh, P., Kumar, A., Sharma, G., Pare, B., Jonnalagadda, S. B. & Thakur, P. 2014 Solar photocatalytic activity of nano-ZnO supported on activated carbon or brick grain particles: role of adsorption in dye degradation. *Applied Catalysis A: General* **486**, 159–169.

Raja, A., Ashokkumar, S., Pavithra Marthandam, R., Jayachandiran, J., Khatiwada, C. P., Kaviyarasu, K., Ganapathi Raman, R. & Swaminathan, M. 2018 Eco-friendly preparation of zinc oxide nanoparticles using *Tabernaemontana divaricata* and its photocatalytic and antimicrobial activity. *Journal of Photochemistry and Photobiology B: Biology* **181**, 53–58.

Rajesh, S., Sagar Reddy Yadav, L. & Thyagarajan, K. 2016 Structural, optical, thermal and photocatalytic properties of ZnO nanoparticles of betel leave by using green synthesis method. *Journal of Nanostructures* **6** (3), 250–255.

Rajkumar, K. S., Arun, S., Dinesh Babu, M., Balaji, P., Sivasubramanian, S., Vignesh, V. & Thirumurugan, R. 2019 Facile biofabrication, characterization, evaluation of photocatalytic, antipathogenic activity and in vitro cytotoxicity of zinc oxide nanoparticles. *Biocatalysis and Agricultural Biotechnology* **22**, 101436.

Rajput, V. D., Minkina, T. M., Behal, A., Sushkova, S. N., Mandzhieva, S., Singh, R., Gorovtsov, A., Tsitsuashvili, V. S., Purvis, W. O., Ghazaryan, K. A. & Movsesyan, H. S. 2018 Effects of zinc-oxide nanoparticles on soil, plants, animals and soil organisms: a review. *Environmental Nanotechnology, Monitoring and Management* **9**, 76–84.

Ramanathan, S., Selvin, S. P., Obadiah, A., Durairaj, A., Santhoshkumar, P., Lydia, S., Ramasundaram, S. & Vasanthkumar, S. 2019 Synthesis of reduced graphene oxide/ZnO nanocomposites using grape fruit extract and *Eichhornia crassipes* leaf extract and a comparative study of their photocatalytic property in degrading Rhodamine B dye. *Journal of Environmental Health Science and Engineering* **17** (1), 195–207.

Rambabu, K., Bharath, G., Banat, F. & Show, P. L. 2021 Green synthesis of zinc oxide nanoparticles using *Phoenix dactylifera* waste as bioreductant for effective dye degradation and antibacterial performance in wastewater treatment. *Journal of Hazardous Materials* **402**, 123560.

Reddy, K. M., Feris, K., Bell, J., Wingett, D. G., Hanley, C. & Punnoose, A. 2007 Selective toxicity of zinc oxide nanoparticles to prokaryotic and eukaryotic systems. *Applied Physics Letters* **90** (21), 10–13.

Rehman, S., Jermy, B. R., Akhtar, S., Borgio, J. F., Abdul Azeez, S., Ravinayagam, V., Al Jindan, R., Alsalem, Z. H., Buhameid, A. & Gani, A. 2019 Isolation and characterization of a novel thermophile; *Bacillus haynesii*, applied for the Green synthesis of ZnO nanoparticles. *Artificial Cells, Nanomedicine and Biotechnology* **47** (1), 2072–2082.

Rupa, E. J., Anandapadmanaban, G., Mathiyalagan, R. & Yang, D. C. 2018 Synthesis of zinc oxide nanoparticles from immature fruits of *Rubus coreanus* and its catalytic activity for degradation of industrial dye. *Optik* **172**, 1179–1186.

Rupa, E. J., Kaliraj, L., Abid, S., Yang, D. C. & Jung, S. K. 2019 Synthesis of a zinc oxide nanoflower photocatalyst from sea buckthorn fruit for degradation of industrial dyes in wastewater treatment. *Nanomaterials* **9** (12), 1692.

Sadik, W. A. 2007 Effect of inorganic oxidants in photodecolourization of an azo dye. *Journal of Photochemistry and Photobiology A: Chemistry* **191** (2–3), 132–137.

Saha, R., Subramani, K., Petchi Muthu Raju, S. A. K., Rangaraj, S. & Venkatachalam, R. 2018 *Psidium guajava* leaf extract-mediated synthesis of ZnO nanoparticles under different processing parameters for hydrophobic and antibacterial finishing over cotton fabrics. *Progress in Organic Coatings* **124**, 80–91.

Saini, R. D. 2017 Textile organic dyes: polluting effects and elimination methods from textile waste water. *International Journal of Chemical Engineering Research* **9** (1), 975–6442.

Saratale, R. G., Saratale, G. D., Chang, J. S. & Govindwar, S. P. 2011 Bacterial decolorization and degradation of azo dyes: *a review*. *Journal of the Taiwan Institute of Chemical Engineers* **42** (1), 138–157.

Satheshkumar, M., Anand, B., Muthuvel, A., Rajarajan, M., Mohana, V. & Sundaramanickam, A. 2020 Enhanced photocatalytic dye degradation and antibacterial activity of biosynthesized ZnO-NPs using curry leaves extract with coconut water. *Nanotechnology for Environmental Engineering* **5** (3), 1–11.

Shabaani, M., Rahaiee, S., Zare, M. & Jafari, S. M. 2020 Green synthesis of ZnO nanoparticles using loquat seed extract; biological functions and photocatalytic degradation properties. *Lwt* **134**, 110133.

Sharma, R., Garg, R. & Kumari, A. 2020 A review on biogenic synthesis, applications and toxicity aspects of zinc oxide nanoparticles. *EXCLI Journal* **19**, 1325–1340.

Sharma, J. L., Dhayal, V. & Sharma, R. K. 2021 White-rot fungus mediated green synthesis of zinc oxide nanoparticles and their impregnation on cellulose to develop environmental friendly antimicrobial fibers. *3 Biotech* **11** (6), 269.

Sheik Mydeen, S., Raj Kumar, R., Kottaisamy, M. & & Vasantha, V. S. 2020 Biosynthesis of ZnO nanoparticles through extract from *Prosopis juliflora* plant leaf: antibacterial activities and a new approach by rust-induced photocatalysis. *Journal of Saudi Chemical Society* **24** (5), 393–406.

Shetti, N. P., Malode, S. J., Malladi, R. S., Nargund, S. L., Shukla, S. S. & Aminabhavi, T. M. 2019 Electrochemical detection and degradation of textile dye Congo red at graphene oxide modified electrode. *Microchemical Journal* **146**, 387–392.

Shim, Y. J., Soshnikova, V., Anandapadmanaban, G., Mathiyalagan, R., Jimenez Perez, Z. E., Markus, J., Ju Kim, Y., Castro-Aceituno, V. & Yang, D. C. 2019 Zinc oxide nanoparticles synthesized by *Suaeda japonica Makino* and their photocatalytic degradation of methylene blue. *Optik* **182**, 1015–1020.

Siddique, K., Shahid, M., Shahzad, T., Mahmood, F., Nadeem, H., Saifur Rehman, M., Hussain, S., Sadak, O., Gunasekaran, S., Kamal, T. & Ahmad, I. 2021 Comparative efficacy of biogenic zinc oxide nanoparticles synthesized by *Pseudochrobactrum* sp. C5 and chemically synthesized zinc oxide nanoparticles for catalytic degradation of dyes and wastewater treatment. *Environmental Science and Pollution Research* **28** (22), 28307–28318.

Singh, B. N., Rawat, A. K. S., Khan, W., Naqvi, A. H. & Singh, B. R. 2014 Biosynthesis of stable antioxidant ZnO nanoparticles by *Pseudomonas aeruginosa* Rhamnolipids. *PLoS ONE* **9** (9), e106937.

Singh, J., Kaur, S., Kaur, G., Basu, S. & Rawat, M. 2019 Biogenic ZnO nanoparticles: a study of blueshift of optical band gap and photocatalytic degradation of reactive yellow 186 dye under direct sunlight. *Green Processing and Synthesis* **8** (1), 272–280.

Singh, A., Verma, A., Singh, R., Sahoo, A. K. & Samanta, S. K. 2021 Combination therapy of biogenic C-dots and lysozyme for enhanced antibacterial and antibiofilm activity. *Nanotechnology* **32** (8), 085104.

Siripireddy, B. & Mandal, B. K. 2017 Facile green synthesis of zinc oxide nanoparticles by *Eucalyptus globulus* and their photocatalytic and antioxidant activity. *Advanced Powder Technology* **28** (3), 785–797.

Siriwardhene, A. 2013 Antihyperglycemic effect and phytochemical screening of aqueous extract of *Passiflora foetida* (Linn.) on normal Wistar rat model. *African Journal of Pharmacy and Pharmacology* **7** (45), 2892–2894.

Sohrabnezhad, S. & Seifi, A. 2016 The green synthesis of Ag/ZnO in montmorillonite with enhanced photocatalytic activity. *Applied Surface Science* **386**, 33–40.

Sorbiun, M., Shayegan Mehr, E., Ramazani, A. & Taghavi Fardood, S. 2018 Green synthesis of zinc oxide and copper oxide nanoparticles using aqueous extract of oak fruit hull (Jaft) and comparing their photocatalytic degradation of basic violet 3. *International Journal of Environmental Research* **12** (1), 29–37.

Soriano, J. J., Mathieu-Denoncourt, J., Norman, G., de Solla, S. R. & Langlois, V. S. 2014 Toxicity of the azo dyes acid Red 97 and Bismarck brown Y to western clawed frog (*Silurana tropicalis*). *Environmental Science and Pollution Research* **21** (5), 3582–3591.

Soto-Robles, C. A., Luque, P. A., Gómez-Gutiérrez, C. M., Nava, O., Vilchis-Nestor, A. R., Lugo-Medina, E., Ranjithkumar, R. & Castro-Beltrán, A. 2019 Study on the effect of the concentration of *Hibiscus sabdariffa* extract on the green synthesis of ZnO nanoparticles. *Results in Physics* **15**, 102807.

Stan, M., Popa, A., Toloman, D., Dehelean, A., Lung, I. & Katona, G. 2015 Enhanced photocatalytic degradation properties of zinc oxide nanoparticles synthesized by using plant extracts. *Materials Science in Semiconductor Processing* **39**, 23–29.

Stiborová, M., Martínek, V., Rýdlová, H., Hodek, P. & Frei, E. 2002 Sudan I is a potential carcinogen for humans: evidence for its metabolic activation and detoxication by human recombinant cytochrome P450 1A1 and liver microsomes. *Cancer Research* **62** (20), 5678–5684.

Sudha, M., Saranya, A., Selvakumar, G. & Sivakumar, N. 2018 Microbial degradation of azo dyes : a review. *International Journal of Current Microbiology and Applied Sciences* **3**, 670–690.

Sur, D. H. & Mukhopadhyay, M. 2019 Role of zinc oxide nanoparticles for effluent treatment using *Pseudomonas putida* and *Pseudomonas aureofaciens*. *Bioprocess and Biosystems Engineering* **42** (2), 187–198.

Suresh, D., Nethravathi, P. C., Udayabhanu, Rajanaika, H., Nagabhushana, H. & Sharma, S. C. 2015 Green synthesis of multifunctional zinc oxide (ZnO) nanoparticles using *Cassia fistula* plant extract and their photodegradative, antioxidant and antibacterial activities. *Materials Science in Semiconductor Processing* **31**, 446–454.

Swen, M. J., Jeanne, D. J., Thomas, R., Peter, E. & Howadrd, I. M. 2020 *Kanerva's Occupational Dermatology*. Springer.

Talebian, N., Amininezhad, S. M. & Doudi, M. 2013 Controllable synthesis of ZnO nanoparticles and their morphology-dependent antibacterial and optical properties. *Journal of Photochemistry and Photobiology B: Biology* **120**, 66–73. http://dx.doi.org/10.1016/j.jphotobiol.2013.01.004.

Talha Khalil, A., Hameed, S., Afridi, S., Mohamed, H. E. A. & Shinwari, Z. K. 2019 *Sageretia thea* mediated biosynthesis of metal oxide nanoparticles for catalytic degradation of crystal violet dye. *Materials Today: Proceedings* **36**, 397–400.

Taran, M., Rad, M. & Alavi, M. 2018 Biosynthesis of TiO_2 and ZnO nanoparticles by *Halomonas elongata* IBRC-M 10214 in different conditions of medium. *BioImpacts* **8** (2), 81–89.

Tripathi, R. M., Bhadwal, A. S., Gupta, R. K., Singh, P., Shrivastav, A. & Shrivastav, B. R. 2014 ZnO nanoflowers: novel biogenic synthesis and enhanced photocatalytic activity. *Journal of Photochemistry and Photobiology B: Biology* **141**, 288–295.

Tunçal, T. 2020 Energy efficient BPA degradation through F_{etched}-Ni-Sn-CN-TiO_2 nano-layered thin film reactors. *Environmental Technology & Innovation* **20**, 101174.

Tunçal, T. & Kaygusuz, T. 2014 Treatment of dyehouse effluents using sequential combinations of electrochemical oxidation, membrane separation, and activated sludge. *Environmental Progress & Sustainable Energy* **33**, 472–481.

Umar, A., Kumar, R., Kumar, G., Algarni, H. & Kim, S. H. 2015 Effect of annealing temperature on the properties and photocatalytic efficiencies of ZnO nanoparticles. *Journal of Alloys and Compounds* **648**, 46–52.

Vandebriel, R. J. & De Jong, W. H. 2012 A review of mammalian toxicity of ZnO nanoparticles. *Nanotechnology, Science and Applications* **5** (1), 61–71.

Varadavenkatesan, T., Lyubchik, E., Pai, S., Pugazhendhi, A., Vinayagam, R. & Selvaraj, R. 2019 Photocatalytic degradation of Rhodamine B by zinc oxide nanoparticles synthesized using the leaf extract of *Cyanometra ramiflora*. *Journal of Photochemistry and Photobiology B: Biology* **199**, 111621.

Venkateasan, A., Prabakaran, R. & Sujatha, V. 2017 Phytoextract-mediated synthesis of zinc oxide nanoparticles using aqueous leaves extract of *Ipomoea pes-caprae* (L).R.Br revealing its biological properties and photocatalytic activity. *Nanotechnology for Environmental Engineering* **2** (1), 1–15.

Ventura-camargo, B. D. C. & Marin-Morales, M. A. 2013 Azo dyes: characterization and toxicity – A review. *Textiles and Light Industrial Science and Technology* **2** (2), 85–103.

Vidya, C., Prabha, M. N. C. & Raj, M. A. L. A. 2016 Green mediated synthesis of zinc oxide nanoparticles for the photocatalytic degradation of Rose Bengal dye. *Environmental Nanotechnology, Monitoring and Management* **6**, 134–138.

Villarreal-Lozoya, J. E., Lombardini, L. & Cisneros-Zevallos, L. 2007 Phytochemical constituents and antioxidant capacity of different pecan [*Carya illinoinensis* (Wangenh.) K. Koch] cultivars. *Food Chemistry* **102** (4), 1241–1249.

Vinayagam, R., Selvaraj, R., Arivalagan, P. & Varadavenkatesan, T. 2020 Synthesis, characterization and photocatalytic dye degradation capability of *Calliandra haematocephala*-mediated zinc oxide nanoflowers. *Journal of Photochemistry and Photobiology B: Biology* **203**, 111760.

Wang, D., Liu, H., Ma, Y., Qu, J., Guan, J., Lu, N., Lu, Y. & Yuan, X. 2016 Recycling of hyper-accumulator: synthesis of ZnO nanoparticles and photocatalytic degradation for dichlorophenol. *Journal of Alloys and Compounds* **680**, 500–505.

Wang, H., Xie, C., Zhang, W., Cai, S., Yang, Z. & Gui, Y. 2007 Comparison of dye degradation efficiency using ZnO powders with various size scales. *Journal of Hazardous Materials* **141** (3), 645–652.

Wang, P., Menzies, N. W., Lombi, E., McKenna, B. A., Johannessen, B., Glover, C. J., Kappen, P. & Kopittke, P. M. 2013 Fate of ZnO nanoparticles in soils and cowpea (*Vigna unguiculata*). *Environmental Science and Technology* **47** (23), 13822–13830.

Weldegebrieal, G. K. 2020 Synthesis method, antibacterial and photocatalytic activity of ZnO nanoparticles for azo dyes in wastewater treatment: a review. *Inorganic Chemistry Communications* **120**, 108140.

Yulizar, Y., Apriandanu, D. O. B. & Ashna, R. I. 2020 La_2CuO_4-decorated ZnO nanoparticles with improved photocatalytic activity for malachite green degradation. *Chemical Physics Letters* **755**, 137749.

Yung, M. M. N., Mouneyrac, C. & Leung, K. M. Y. 2014 Ecotoxicity of zinc oxide nanoparticles in the marine environment. In: *Encyclopedia of Nanotechnology*, (Bhushan B., eds.), Springer, Dordrecht, pp. 1–17.

Zaidi, Z., Siddiqui, S. I., Fatima, B. & Chaudhry, S. A. 2019 Synthesis of ZnO nanospheres for water treatment through adsorption and photocatalytic degradation: modelling and process optimization. *Materials Research Bulletin* **120**, 110584.

Zhang, H., Yang, D., Ji, Y., Ma, X., Xu, J. & Que, D. 2004 Low-temperature synthesis of flower like ZnO nanostructures by cetyltrimethylammonium bromide-assisted hydrothermal process. *Journal of Physical Chemistry B* **108** (13), 3955–3958.

Zhang, F., Chen, X., Wu, F. & Ji, Y. 2016 High adsorption capability and selectivity of ZnO nanoparticles for dye removal. *Colloids and Surfaces A: Physicochemical and Engineering Aspects* **509**, 474–483.

Zhu, X., Pathakoti, K. & Hwang, H.-M. 2019 Green synthesis of titanium dioxide and zinc oxide nanoparticles and their usage for antimicrobial applications and environmental remediation. In: *Green Synthesis, Characterization and Applications of Nanoparticles*, (Sukhla, A. K. & Iravani, S., eds.). Elsevier Inc., pp. 223–263.

First received 12 June 2021; accepted in revised form 17 September 2021. Available online 29 September 2021